Geologica Acta, Vol.5, Nº 3, 2007, 199-230
Available online at www.geologica-acta.com

Statistical grid-based facies reconstruction and modelling for sedimentary bodies. Alluvial-palustrine and turbiditic examples

O. FALIVENE|1|* **L. CABRERA**|1| **J.A. MUÑOZ**|1| **P. ARBUÉS**|1| **O. FERNÁNDEZ**|2| **and A. SÁEZ**|1|

|1| **Geomodels-Group of Geodynamics and Basin Analysis, Universitat de Barcelona. Dpts. EPGM and GG.**
c/ Martí i Franquès, s/n, Facultat de Geologia, 08028 Barcelona, Spain.

|2| **Midland Valley Inc,**
1767A Denver West Blvd., Golden CO 80401, USA

* Corresponding author present address: BP Exploration Company Limited, Building H, EPT Geological Services, Chertsey Road, Sunbury on Thames, Middlesex TW16 7, United Kingdom. E-mail: Oriol.Falivene@bp.com

ABSTRACT

The geological community is increasingly aware of the importance of geological heterogeneity for managing subsurface activities. In sedimentary bodies, facies distribution is an important factor constraining geological heterogeneity. Statistical grid-based sedimentary facies reconstruction and modelling methods (FRM methods) can be used to provide accurate representations (reconstructions or models) of facies distribution at a variety of scales, which can be conditioned to hard and soft data. These representations enable geological heterogeneity to be quantified; and therefore, serve as important inputs to manage projects involving subsurface activities. FRM methods are part of a general workflow comprising the construction of a surface-based framework, which is used to build the modelling grid in which these methods operate. This paper describes this workflow and provides an overview, classification, description and illustration of the most widely used FRM methods (deterministic and stochastic). Among others, two selected datasets comprising alluvial-palustrine and turbiditic deposits are used for illustration purposes. This exercise enables critical issues when using FRM methods to be highlighted and also provides some recommendations on their capabilities. For deterministic facies reconstruction, the main choice of the method to be used is between that employing a continuous or a categorical method. For stochastic facies modelling, choosing between the different techniques must be based on the scale of the problem, the type and density of available data, the objective of the model, and the conceptual depositional model to be reproduced. Realistic representations of facies distribution can be obtained if the available methods are applied appropriately.

KEYWORDS | **Facies model. Facies reconstruction. Mathematical models. Sedimentary heterogeneity.**

INTRODUCTION

Utility of facies reconstruction and modelling methods

Valid representations of geological heterogeneity are important inputs for quantitative models used in managing subsurface activities. In sedimentary bodies, facies distribution is an important factor constraining sedimentological and therefore geological heterogeneity. The recognition of facies distribution in the subsurface by using direct methods, such as continuous core recovery boreholes, is expensive and can only be afforded to directly investigate very restricted areas.

© UB-ICTJA

The use of indirect methods, such as geophysical logs or seismic image provides information covering larger areas, although with less resolution or accuracy. Additional geological information, such as conceptual depositional models, regional geology, paleogeographic maps or sedimentation rates, can also be useful for constraining facies distribution in the subsurface. Aiming to optimise the use of geological data, several modelling approaches for creating images of sedimentary heterogeneity in the subsurface exist. Most currently used methods can be classified within two main categories: structure-imitating and process-imitating. Structure-imitating approaches numerically reproduce the observed spatial patterns without directly considering sedimentary processes (Koltermann and Gorelick, 1996). Process-imitating or process-based approaches are focused towards the direct mathematical formulation and simulation of the physical processes controlling the erosion, transport and accumulation of sediments (Tetzlaff and Harbaugh, 1989; Koltermann and Gorelick, 1996).

Statistical grid-based facies reconstruction and modelling methods (named hereafter as FRM methods for simplicity) are referred herein to group those structure-imitating methods based on deterministic or probabilistic rules, operating on a grid and designed to build facies reconstructions or models. These methods are able to provide detailed representations of facies distribution in the subsurface that honours a wide range of input information, allows a rapid correlation, visualization and comprehension of the facies distribution, and serves as a starting point for further applications. FRM methods are part of a more general facies reconstruction and modelling workflow, which also includes the construction of a surface-based framework and the grid design.

Many geological disciplines employ FRM methods; among the most important are the natural resource exploitation, the storage of residual or strategic substances in the subsurface, and the planning of civil engineering projects. For example, in the oil industry and hydrogeology the detailed representation of facies in the reservoir or the aquifer is used as the starting point for volumetric or connectivity analysis (Mijnssen, 1997; Knudby and Carrera, 2005). Wherever a correlation between petrophysical parameters and facies can be established, facies representation can be used as an input to petrophysical modelling and subsequent flow simulation (Deutsch and Hewett, 1996; de Marsily et al., 2005). Other typical applications are related to the mining industry, where FRM methods are used to constraint the extension, thickness, quality and exploitability of resources (Journel and Huijberts, 1978; Journel and Isaaks, 1984).

An increasing number of FRM methods are currently available. Detailed reviews dealing with some of these methods can be found in Haldorsen and Damsleth (1990), Srivastava (1994), Koltemann and Gorelick (1996), de Marsily et al. (1998) and Webb and Davis (1998). It is important to note that research has traditionally focused on showing the possibilities and pitfalls of each method, whereas much work still needs to be done in terms of comparing the performance of these methods when applied to real datasets (de Marsily et al., 2005).

Aims

This paper presents an overview of the general workflow for the reconstruction and modelling of facies distribution by using FRM methods. FRM methods are introduced, relevant applications of these methods in the published literature are outlined, and then the procedures for obtaining facies distributions are explained and illustrated by applying them to two selected datasets. One dataset derives from an alluvial to palustrine-lacustrine coal-bearing interval in the As Pontes basin (Oligocene, NW Spain) and the other from a turbidite channel-fill in the Ainsa basin (Eocene, NE Spain). Both datasets present differences related to data format, data spacing, and scale of heterogeneities to be reproduced, enabling illustration of a wide range of FRM methods.

The As Pontes dataset is composed of closely spaced coal exploration wells. The objective of the FRM methods applied to this dataset is to generate facies reconstructions able to predict overall facies distribution patterns by integrating all facies descriptions recorded at the wells. This dataset is therefore used to illustrate deterministic facies reconstruction methods.

The Ainsa dataset comprises an outcrop characterization resolving facies distribution at bed-scale. The objective of the FRM methods applied to this dataset is to generate facies distributions resembling the spatial patterns observed at the outcrop. This dataset is therefore used to illustrate stochastic facies modelling methods.

The application of FRM methods to the selected datasets enabled critical issues on facies modelling to be highlighted, and the applicability of each FRM method to be assessed. It is important to note that the aim of this paper is not to cover all the available FRM methods developed previously; it is instead to focus on selected and useful methods that have been demostrated to be successful in many cases and are currently widely used.

FACIES RECONSTRUCTION AND MODELLING WORKFLOW

The starting assumption in the facies reconstruction and modelling workflow is that sedimentary heterogeneity can be described in hierarchical elements of diverse scales (Weber, 1986; Van de Graaf and Ealey, 1989; Miall, 1991; Huggenberger and Aigner, 1999; Fig. 1). Typically, facies modelling proceeds from the larger to the smaller scale of heterogeneity (Hurst et al., 1999; Hurst et al., 2000), and is usually applied to resolve from mega- to macro-scale. Giga-scale and mega-scale facies heterogeneity are better suited to description using a deterministic surface-based framework (see below), whereas FRM methods typically better represent the macro-scale facies heterogeneity, even though this can vary depending on the objective of the facies reconstruction or model, the input data available, or the complexity of the subsurface heterogeneity. Meso-scale heterogeneity is sometimes approached directly by petrophysical modelling methods, by FRM methods, or more recently by innovative non grid-based, genetically based unconditioned facies modelling methods (Scheibe and Freyberg, 1995; Pyrcz et al., 2005; Ringrose et al., 2005). Micro-scale heterogeneity is usually the subject of petrophysical modelling methods (Dubrule and Haldorsen, 1986; MacDonald et al., 1992; Goovaerts, 1999; Willis and White, 2000; Deutsch, 2002; Stephen et al., 2002; Hauge et al., 2003; Larue 2004; Larue and Legarre, 2004; Larue and Friedmann, 2005; Pyrcz et al., 2005).

The general workflow for grid-based reconstruction and modelling of facies distribution in sedimentary bodies using FRM methods involves three consecutive steps (Jones, 1988; Krum and Johnson, 1993; Dubrule and Damsleth, 2001; Fig. 2): 1) the construction of a surface-based framework; 2) the definition of modelling grids, constrained by the surfaces reconstructed previously; and 3) the assigning of facies to each cell using FRM methods. It is important that a robust depositional conceptual model can be established previously from regional geological information and available input data (Weber and van Geuns, 1990). This model will mainly serve for guiding basic decisions during the reconstruction and modelling workflow (i.e. the detail of correlation that can be deterministically resolved, appropriateness of the different FRM methods, grid design, selection of analogues or modelling scenarios, etc.).

Surface-based framework

The first step in the facies reconstruction and modelling workflow is the definition of the volume of interest by means of top and bottom surfaces (Fig. 2A). Depending on the complexity of heterogeneity and sample data spacing, additional extensive and correlatable surfaces lying within this volume can be also constructed, providing a more detailed subdivision of the system (Fig. 2A). The main objective of this step is to identify and separate genetic units characterized by the occurrence and distribution characteristics of the different facies. Ideally, the

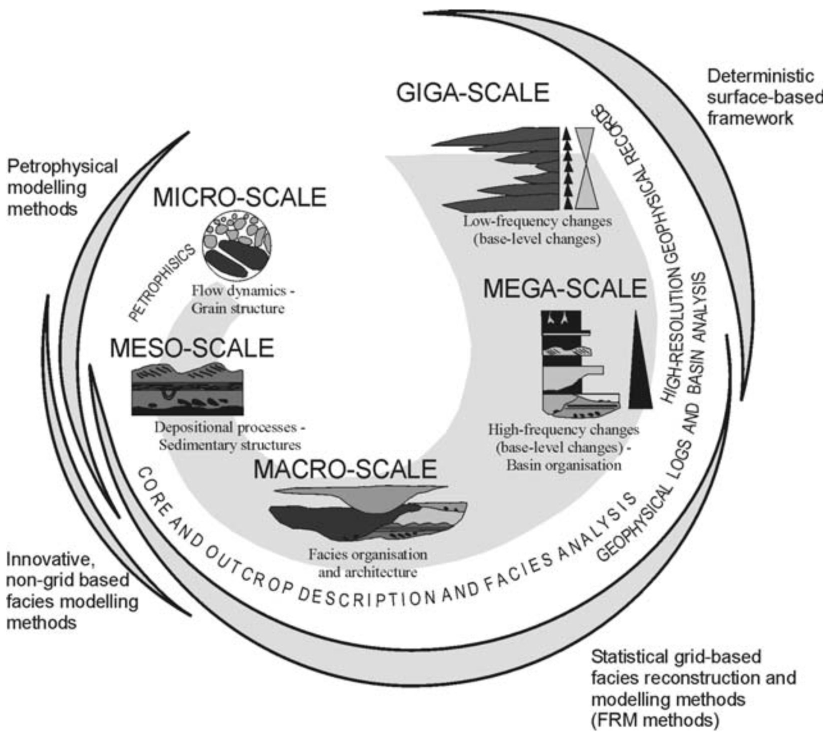

FIGURE 1 | **Sedimentological heterogeneity scales, origins, study techniques (modified from Heinz and Aigner, 2003), and geological modelling strategies. See text for detailed explanation.**

surface-based subdivision would separate units that could be considered as stationary (i.e. whose statistical properties do not vary significantly throughout the unit), in order to facilitate the subsequent facies reconstruction and modelling. However, this is usually not achieved, due to lack of data or the presence of intrinsic non-stationarities in the depositional system; in these cases the reconstruction or modelling process should take into account the presence of trends in facies distribution and facies characteristics. This first step can be of great complexity (MacDonald et al., 1998; Artimo et al., 2003; Fernández et al., 2004; Ross et al., 2005; Arbués et al., in press; Falivene et al., 2006c) and its description could be the subject of a paper by itself. However, this step is not described here in further detail, as this paper concentrates on the FRM methods.

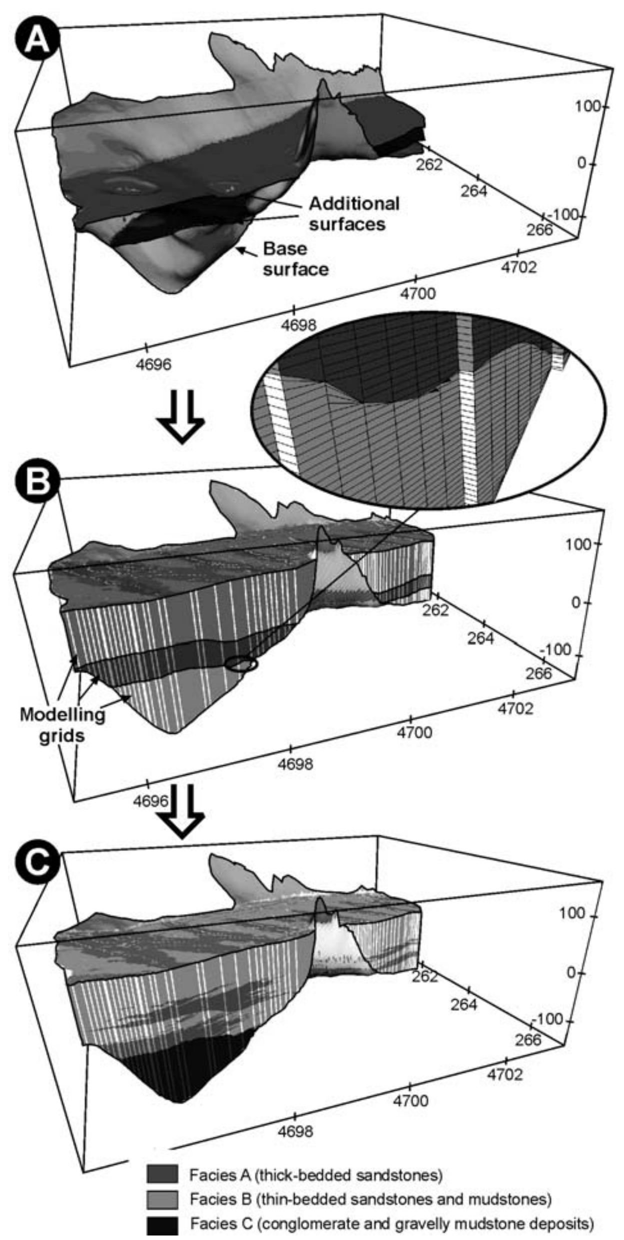

FIGURE 2 **Example showing the three phases of the general workflow for grid-based statistical reconstruction and modelling of facies distribution. A) Surface-based framework. B) Modelling grids constructed between stratigraphically consecutive surfaces, note the detail showing cell arrangement. C) Facies assigned to grid cells. This example corresponds to the Morillo Turbidite System (Ainsa Basin slope complex, NE Spain), and was reconstructed mostly by using outcrop data (Arbués et al., 2003). Vertical exaggeration is 10x and the vertical coordinates datum corresponds to a paleodepositional surface (Fernández et al., 2004). Heights are expressed in metres. Horizontal coordinates are in km in Universal Transverse Mercator (UTM) zone 31.**

Modelling grid

The second step uses the surfaces described previously to design the modelling grids, which are the necessary support for FRM methods. Two stratigraphically consecutive surfaces define the base and the top of each modelling grid (Fig. 2B).

Each modelling grid consists of a number of adjacent cells, usually parallelepipeds, to which facies are assigned. The sides of the cells are commonly vertical and define a rectangular mesh as seen in map view, whereas bases and tops (i.e. the grid layering) may differ from the horizontal. Grid layering is defined to mimic those planes where facies should display more continuity (i.e. paleodepositional surfaces or bedding planes; Jones, 1988, 1992). It reproduces tectonic and sedimentary geometries such as onlap, offlap, burial effects and erosion (Fig. 3), according to the previous geological knowledge and the conceptual depositional model. However, FRM methods work on rectangular grids in order to speed up distance calculations, and this is achieved during the modelling stage by temporally flattening grid layering to horizontal and planar surfaces.

Grid layering style has a large impact on the results obtained by FRM methods (Ainsworth et al., 1999; Falivene et al., 2007). Horizontally, the modelling grid should be designed with one of its axes aligned with the most important anisotropy direction; this optimises the number of cells necessary to capture the sedimentary heterogeneity (Weber and van Geuns, 1990).

Assigning of facies to grid cells

The assigning of a facies category to each grid cell corresponds, *sensu strictu*, to the facies reconstruction and modelling process (Fig. 2C). Some information regarding input data types and FRM methods classification should be introduced before approaching the different methods.

Input data classification

Data from different sources are integrated by FRM methods. Input data can be classified into two main types:

a) Hard data refer to facies observed at certain positions and most usually derive from well logs or stratigraphic sections (Falivene et al., 2006b). A model is conditioned by hard data when these data are reproduced by the model; this means that cells intersected by or containing hard data information are assigned the observed facies at that point. This process requires scaling-up the original hard data to the grid resolution (Fig. 4). In most cases, facies boundaries identified in the logs do not correspond with the limits of grid cells, and therefore more than one facies category may be present in a cell; since assigning more than one facies category to an individual cell is not possible, an averaging must be performed (i.e. up-scaling of log data; Satur et al., 2005). Usually the category with the largest occurrence within the cell is chosen as the most representative (Fig. 4). The process of log data scaling to the size of the grid cells may result in differences between facies proportions and distribution observed in the original log data, and the up-scaled hard data. Nevertheless, if the dimensions of the modelling grid cells are sufficiently small with respect to the resolution of the facies descriptions in the original data, this bias will not be significant for further facies modelling operations (Fig. 4). Intersected cells represent only a small fraction of all the modelling grid, and the final objective of the FRM methods is to assign a facies to each non-intersected cell.

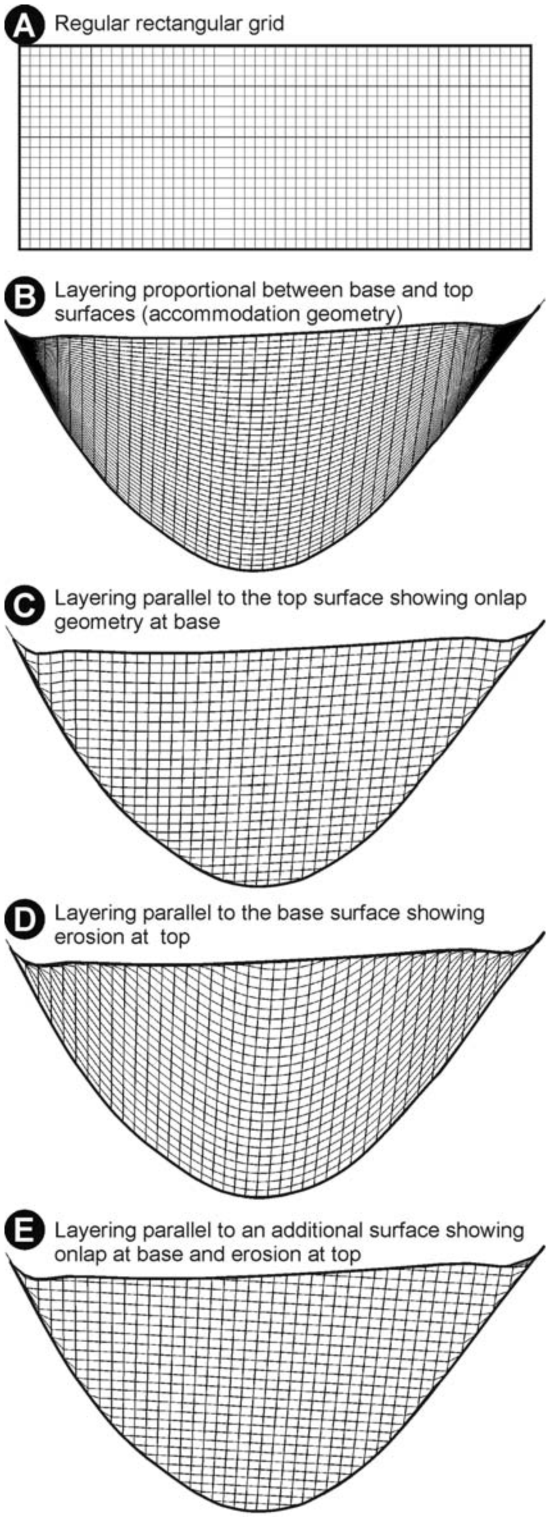

FIGURE 3 | **Grid layering styles as seen in a vertical section of a sedimentary body. A) Regular rectangular grid. B to E) Irregular grids with layering style reproducing different infill layering architectures.**

b) Soft data are not as univocally linked to geographic positions as hard data, and serve as auxiliary conditioning data. Each method uses different types of soft data; typical examples correspond to statistical and geological parameters constraining facies continuity (proportions, variations in proportions, variograms, training images, object characteristics, etc.) and conceptual depositional models. Soft data refers also to indirect measurements, typically carried out by means of geophysical methods, that can be calibrated to facies occurrence, and inform about the gross facies distribution (Mao and Journel, 1999; Yao, 2002; Liu et al., 2004). In subsurface modelling studies, in which the soft data extracted from the available information are not sufficiently constrained for input to FRM methods, it is common practice to also consider information derived from other geologically-similar better-documented examples, i.e. analogues (Alexander, 1993; Bryant et al., 2000; Dalrymple, 2001). This has led to the compilation of databases containing geological descriptions and soft data parameters, either derived from rock record analogues (e.g. Bryant and Flint, 1993; Dreyer et al., 1993; Falkner and Fielding, 1993; Hornung and Aigner 1999; Robinson and McCabe, 1997; Dalrymple, 2001; Pringle et al., 2004; de Marsily et al., 2005; Falivene et al., in press), modern depositional systems (e.g. Tye, 2004), laboratory experiments or genetically based models (e.g. Clementsen et al., 1990; Bridge and Mackey, 1993; Doligez et al., 1999).

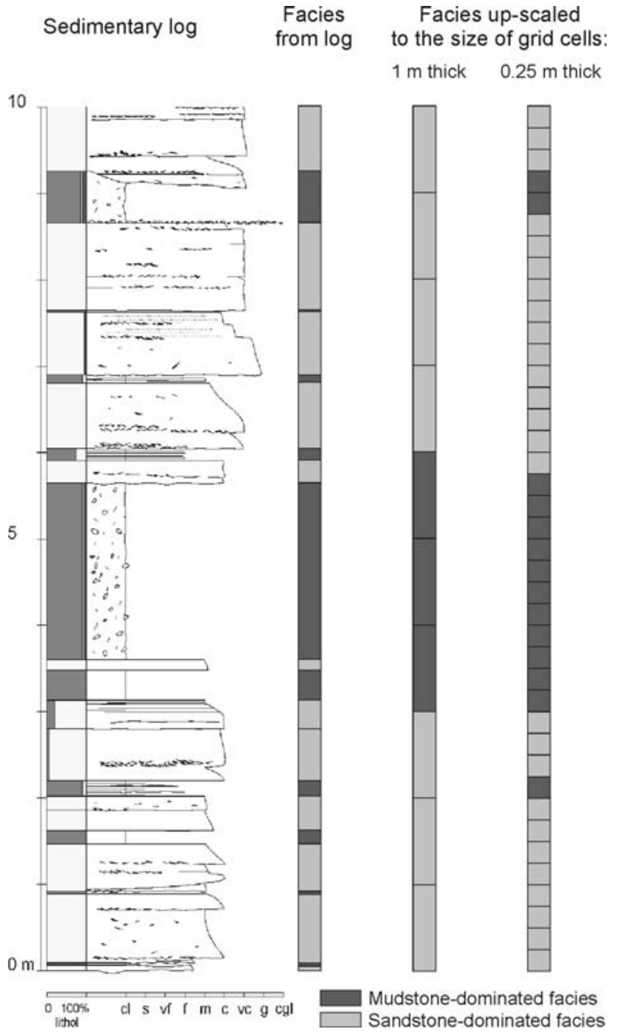

FIGURE 4 | **Sketch illustrating the process of up-scaling of hard data information to the size of grid cells. Results considering different cell thicknesses are shown. Note that the coarser the grid, the lower the resolution obtained.**

Classification of statistical grid-based facies reconstruction and modelling methods

FRM methods can be classified according to the objective of the resultant facies distribution, and the general procedure for obtaining the facies distribution (Fig. 5).

Deterministic versus stochastic methods

According to the purpose of FRM methods, two groups can be established (Fig. 5):

a) Deterministic methods provide a facies reconstruction, which is a unique and smooth solution aiming at local accuracy (Isaaks and Srivastava, 1989; Journel et al., 2000; Fig. 6). Facies reconstructions are based on interpolation algorithms and provide estimates of the most probable facies category at each grid node. In practice, facies reconstructions are only useful in settings where hard data are abundant with respect to sedimentary heterogeneity. The following characteristics are common to all the deterministic methods: 1) facies estimated at each grid cell is obtained independently of the facies estimated at the other cells; 2) the histogram of the reconstructed property is different from that of the original hard data (i.e. lower standard deviation); in terms of facies reconstruction this implies that the resulting facies proportions differ from the original ones, with the proportions of the most extended categories being increased; 3) spatial continuity (measured in terms of variogram ranges) of the resulting facies reconstruction is also increased with respect to that of the original hard data (i.e. smoothing effect, Isaaks and Srivastava, 1989; Journel et al., 2000); 4) the strongest control on the reconstructed facies distribution is exerted by hard data, although a restricted influence related to soft data is also present (e.g. Falivene et al., in press); and 5) facies reconstructions are always conditioned by hard data (i.e. they honour hard data).

b) Stochastic methods provide a set of facies models (i.e. realizations, Fig. 6) with equiprobable facies distributions. In each model all the facies heterogeneity is represented aiming at reproducing global accuracy (i.e. reproduce the entire spatial structure and variability of facies distribution), even though the exact distribution of facies heterogeneities cannot be totally identified with the hard data. Representing all the facies heterogeneity is accomplished by the use of algorithms incorporating random numbers, which are sampled from probability distribution functions (i.e. functions assigning to every possible outcoming value a probability of occurrence, PDF). Facies models are useful when heterogeneity is not sufficiently restricted by hard data, but should be realistically represented to enable a realistic assesment of properties that are influenced by the whole facies distribution (i.e. flow-related responses). The following characteristics are common to all the stochastic methods: 1) facies estimated at each grid cell directly depends, at least partially, on the facies estimated at the other cells; 2) the histogram for the resulting modelled property (or facies proportions) is controlled by soft data, and can reproduce that of the original hard data; 3) spatial continuity of the resultant facies model is also controlled by soft data, and can reproduce that of the original hard data; 4) the main control on the modelled facies distribution is exerted by soft data (Fig. 6); and 5. Facies reconstructions can be either conditioned by hard data (i.e. they honour hard data), or not.

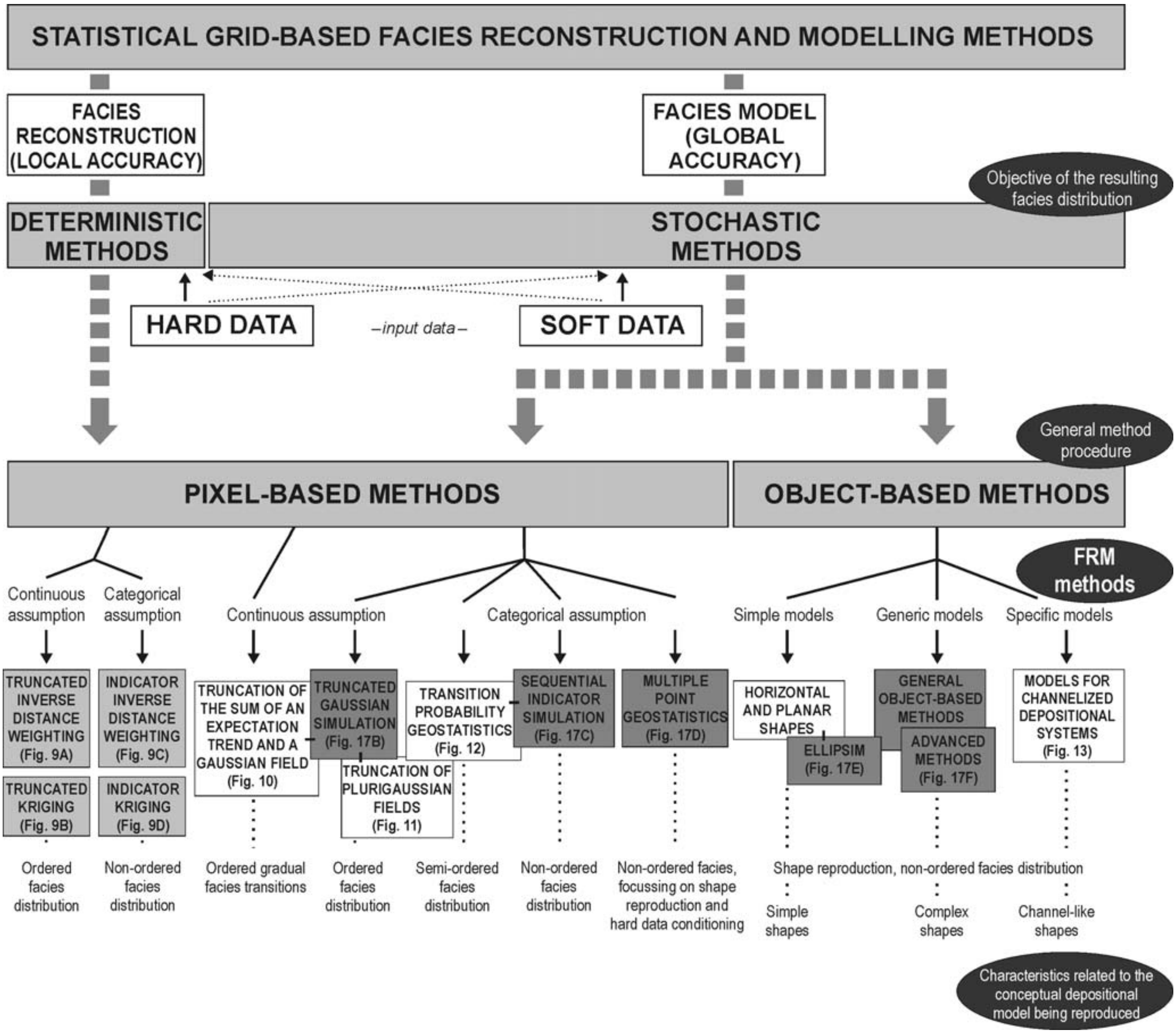

FIGURE 5 | **Scheme for the classification and use of statistical grid-based facies reconstruction and modelling methods (FRM methods). The methods are classified according to the resultant facies distribution purpose and the general method procedure. FRM methods illustrated with the As Pontes basin dataset are included in light grey boxes. Methods illustrated with the Ainsa basin dataset are included in dark grey boxes. Other examples have been used to illustrate those methods included in white boxes. The characteristics related to the conceptual depositional model being reproduced are also shown. See text for detailed discussion on each FRM method.**

Pixel-based versus object-based methods

According to the general procedure for dealing with facies reconstruction and modelling, FRM methods can be subdivided in two different groups (Fig. 5):

a) Pixel-based methods assign a facies to grid cells according to the facies occurrence PDF, which is computed for each grid cell. These methods allow direct conditioning by hard data. The different methods within this group differ in the assumptions made to compute the facies occurrence PDF : continuous or categorical. Continuous methods are based on transforming facies categories to a continuous property (i.e. a property which takes real values ordered from the smallest to the largest), reconstructing or modelling the distribution of the continuous property over all the grid cells, and truncating this property using several thresholds in order to obtain the categorical facies distribution (e.g. Rudikiewicz et al., 1990). Categorical methods are based on transforming each facies category to a new property, defined as the occurrence probability of the facies, and building the PDF at each grid cell as the combination of the reconstruction or modelling of these new properties (e.g. Journel and Alabert, 1989).

b) Object-based methods are characterized by the introduction of objects replacing a background, which commonly represents the most laterally extensive facies. This approach is called also Boolean (e.g. Delhomme and Giannesini, 1979; Haldorsen and Chang, 1986). Objects are assigned a facies, have a predefined geometry, and are introduced until a set of conditions is met. Geometries and conditions depend upon the particular algorithm and algorithm set up; these should be based on the conceptual depositional model. Geometries are defined using a PDF for each object parameter. Among conditions, facies proportions are generally considered to be the most critical. Then, the objects are discretized according to the grid geometry and thus each object may span a number of cells. Conditioning to hard data is frequently achieved through the implementation of iterative algorithms, this can be time-consuming, and in some cases yields non-converging solutions, with conditioning artifacts near hard data.

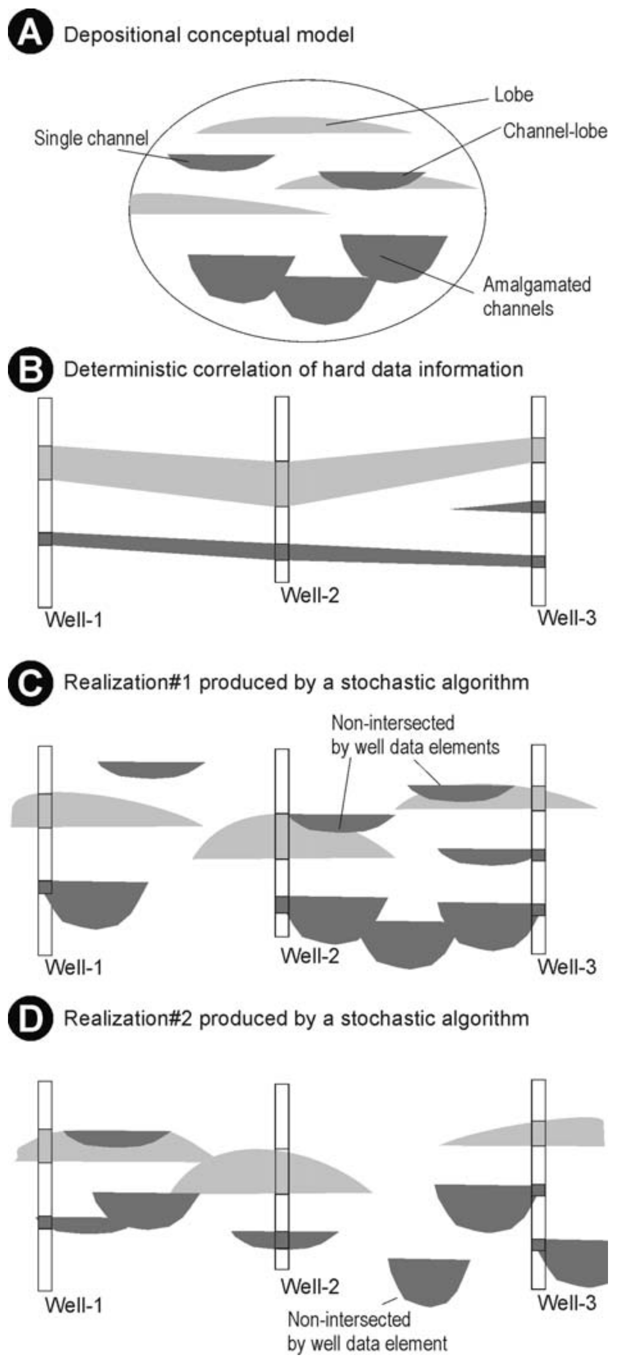

FIGURE 6 | **Sketch comparing facies distributions obtained by a deterministic reconstruction method (B), and two conditioned realizations of a stochastic modelling method: (C) and (D). The deterministic reconstruction is based mainly on well data (hard data). The stochastic model assumes that hard data do not capture all the heterogeneity present; and incorporates the missing heterogeneity based on the conceptual depositional model (A), which is parameterised into into soft data.**

All the deterministic methods are included within the pixel-based group, whereas stochastic methods can fit either within pixel-based or object-based groups. All the object-based methods are stochastic methods, whereas pixel-based methods include either deterministic or stochastic methods (Fig. 5).

DETERMINISTIC FACIES RECONSTRUCTION METHODS

In order to illustrate deterministic FRM methods, the results obtained from reconstructing the first dataset are used. This dataset derives from alluvial-palustrine deposits in the As Pontes basin (NW Spain). Examples on the use of deterministic facies reconstruction methods in the literature will be introduced before presenting the application of the different methods to the As Pontes dataset.

Background on the use of deterministic facies reconstruction methods

The use of deterministic methods for obtaining facies reconstructions has not been as widespread in the literature as the use of stochastic methods for obtaining facies models (see below). Johnson and Dreiss (1989) and Ritzi et al. (1995) applied a deterministic categorical method (Indicator Kriging: IK; Fig. 5) to obtain facies reconstructions in clastic aquifers, in both cases with only two different facies categories, making the results of this method very similar to those obtained with a continuous method. Falivene et al. (in press) used a categorical method (IK) to reconstruct facies distribution in a fine-grain alluvial fan. Moreover, Falivene et al. (2007) compared visually and statistically several facies reconstruction methods (Truncated Inverse Distance Weighting: TIDW, Truncated Kriging: TK, Indicator Inverse Distance Weighting: IIDW, and Indicator Kriging IK [Fig. 5], among others) applied to a heterogeneous coal seam, this work was based on the same dataset as here. Other studies have focused on deterministic reconstructions of continuous parameters that can directly be related to facies (mud fraction in Flach et al. [1998]; grain-size compositions in Koike et al. [1998]; or results of geotechnical cone penetration tests in Lafuerza et al. [2005]). This approach is conceptually similar to continuous methods for facies reconstruction (TK and TIDW). In all cases, published facies reconstructions achieved by deterministic methods have been derived from extensively sampled sites.

The scarcity of deterministic facies reconstructions in the literature (compared to stochastic facies models, see below) is due to: a) the lack of digital high-density (with respect to facies heterogeneity) detailed facies descriptions; and b) the smoothing effect of deterministic methods (Isaaks and Srivastava, 1989; Olea and Pawlowsky, 1996; Journel et al., 2000; Yamamoto, 2005), which results in facies reconstructions yielding usually optimistic results compared to the real heterogeneity distribution (i.e. more homogeneous distributions), limiting their predictive use. Moreover, as the density of the dataset with respect to facies heterogeneity decreases, the smoothing effect of facies reconstructions increases.

Application of facies reconstruction methods to the As Pontes basin dataset

Introduction

The As Pontes basin is a small non-marine basin (12 km^2) resulting from the activity of an Oligocene-Early Miocene strike-slip fault system (Santanach et al., 1988, 2005; Fig. 7A). During the early evolutionary stages of this system, two sub-basins bounded by contractional and extensional structures developed (Eastern and Western) (Ferrús, 1998; Santanach et al., 2005; Figs. 7B and 7C). The basin-fill in both sub-basins resulted from the interaction of sedimentation in alluvial fans and lacustrine to marsh-swamp systems, and consists of siliciclastic facies assemblages together with significant coal deposits (Bacelar et al., 1988; Cabrera et al., 1995, 1996; Ferrús, 1998). The dataset used herein is comprised of 174 coal exploration wells drilling the 6AW coal zone in the western subbasin (Ferrús, 1998; Fig. 7C). The available continuous core descriptions record beds thicker than 0.15 m with a total length of 4000 m. Well placement approximates a regular grid, spaced at about 105m (Fig. 7D). The 6AW coal zone is made up of coal facies interfingering with lacustrine and alluvial mudstone facies, it extends over 2.5 km^2, and averages 30 m in thickness, with its maximum thickness towards the northern active basin margin (50 m).

Owing to the high density of information in the As Pontes dataset, this dataset was deemed useful to illustrate and compare the results obtained by different deterministic pixel-based facies reconstruction methods (Fig. 5); the objective of these methods is to generate facies recons-

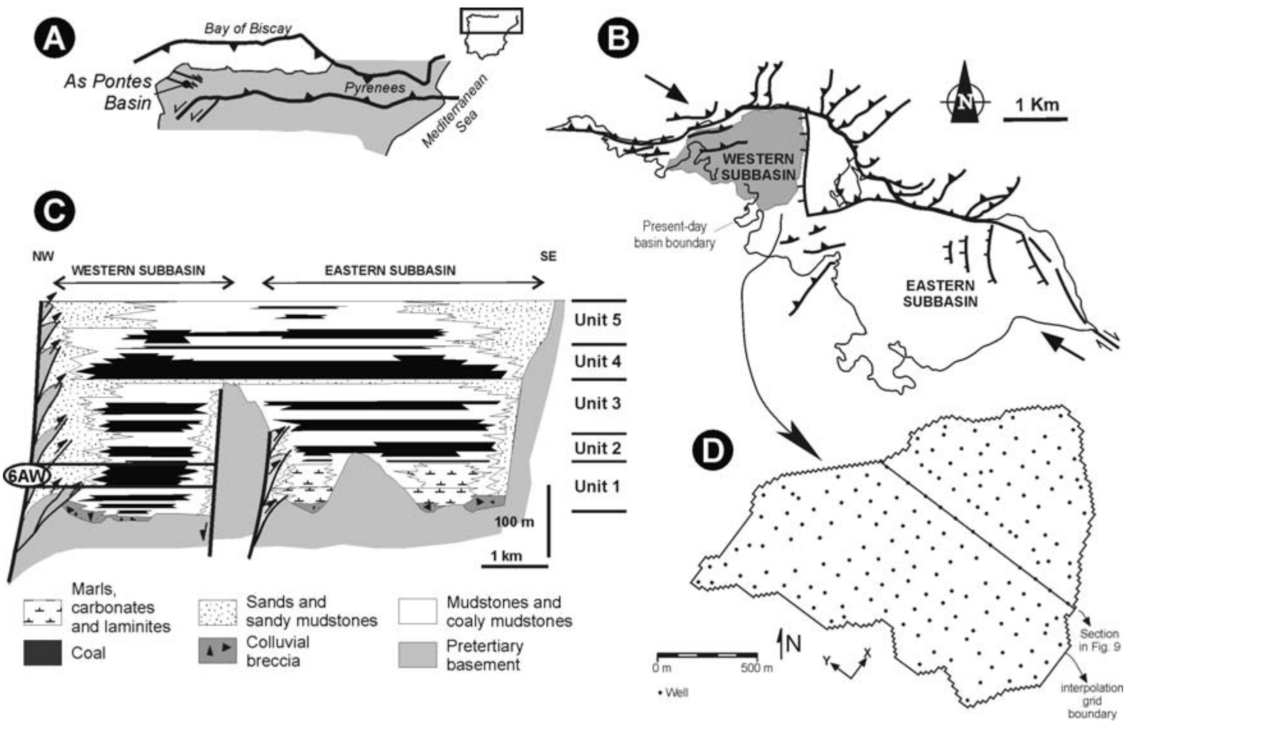

FIGURE 7 | **A) Location of the As Pontes basin. B) Geological map of the basin showing the main tectonic structures that affect the basement. Note the strike-slip fault and associated thrusts, which bound the northern basin margin; the N–S oriented normal faults and the E–W and NE–SW oriented thrusts. C) Longitudinal sketch of the basin showing the main stratigraphic units, sedimentary facies and basement structures (see arrows for location on frame B). Note the stratigraphic position of the 6AW coal zone. D) Well location in the studied part of 6AW zone. The studied part corresponds to the grey shaded zone in frame B. Location of the NW-SE section in Figure 9 is shown.**

tructions able to predict the overall facies distribution patterns by integrating all well data. Both continuous methods (TK and TIDW) and categorical methods (IK and IIDW) were employed.

General set up

For facies reconstruction purposes, the top of the coal zone was considered as an isochrone surface and used as a horizontal datum. This allowed to remove most of the tectonic deformation along the northern basin margin (Santanach et al., 2005), and enabled and improved visualization of facies distribution results. The grid layering style was set up as proportional between the flattened top of the coal zone and a lower surface. In the inner parts and active margin of the basin the lower surface coincided with the base of the coal zone, enabling reproduction of post-depositional deformed geometries. In the passive basin margin the lower surface was set nearly horizontal, and this in combination with the inclined geometry of the base of the coal zone, which dips towards the inner basin parts, enabled the reproduction of an onlap pattern typical of expansive coal zones like 6AW (for details see Falivene et al., 2007). Horizontal grid spacing was set to 20 m; vertical grid spacing varied due to the use of a proportional grid layering style (see example in Fig. 3B), but was set with an average of 0.15 m.

Hard data corresponded to the facies descriptions recorded in the wells. For facies reconstruction purposes, five facies categories were used: lacustrine mudstones (LM), dark brown coal (DBC), pale yellow brown coal (PBC), xyloid brown coal (XBC) and alluvial mudstones (AM). These facies have been described elsewhere (Cabrera et al., 1992, 1995; Hagemann et al., 1997; Huerta et al., 1997; Huerta, 1998, 2001). Facies logs were upscaled to the size of grid cells by assigning the most abundant logged facies to each grid cell intersected by hard data (see example in Fig. 4). Owing to the high density of data, it was possible to extract soft data from the upscaled hard data; these data included proportions (3% for LM, 12% for PBC, 53% for DBC, 7% for XBC and 25% for AM), geometric anisotropy factors, variograms, indicator anisotropy factors and indicator variograms (Tables 1 and 2; Falivene et al., 2007).

Truncated Kriging and Truncated Inverse Distance Weighting (continuous methods)

Preliminary data transformations

The first step in continuous methods for facies reconstruction (Fig. 5) is the transformation of facies categories to a continuous property. This requires preliminary facies ordering based on the conceptual depositional model. In the As Pontes example facies were ordered following transport energy-related paleoenvironment criteria (LM, PBC, DBC, XBC and AM; Fig. 8). Continuous methods start by calculating the thresholds between facies; assuming a Gaussian distribution for the continuous facies property function, the areas between thresholds correspond to the measured proportions in the hard data (Fig. 8). The next step is to assign to each facies a value between their thresholds. In the As Pontes case, constant values located in the centre of each category were used, which is a common practice (Fig. 8; Deutsch, 2002).

Interpolation algorithm and results

Once the facies categories are assigned a continuous property value, facies reconstruction proceeds with the interpolation of the continuous property over the modelling grid nodes. Interpolation estimates the most probable value at each grid node; and therefore, it is not necessary to compute the entire PDF of facies occurrence for each grid node.

Several algorithms have been used for estimating the most probable value of a continuous property at non-sampled locations from a few scattered hard data (see examples in Weber and Englund, 1992, 1994; Dirks et al., 1998; Zim-

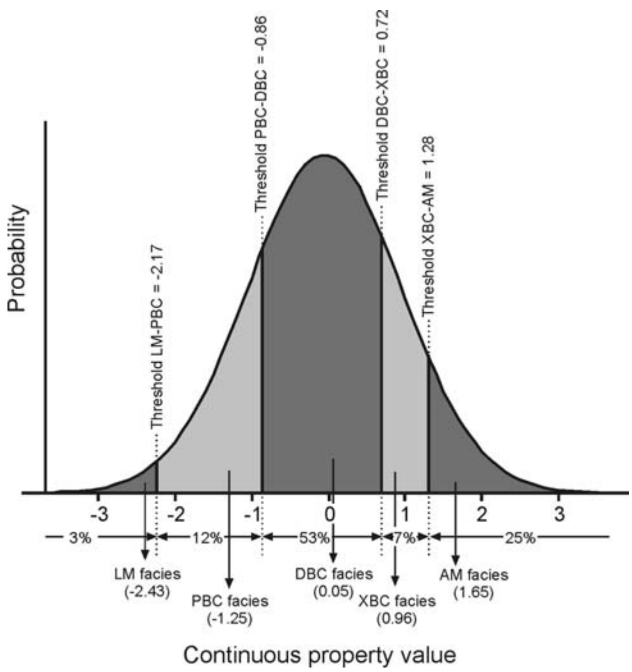

FIGURE 8 **Illustration of the transformation of facies categories to a continuous variable assuming a gaussian distribution for the As Pontes dataset. Note the proportions of each facies, the thresholds between facies categories, and the values of the continuous property assigned to each facies in brackets. LM stands for lacustrine mudstones, PBC for pale brown coal, DBC for dark brown coal, XBC for xyloid brown coal and AM for alluvial mudstones.**

merman et al., 1999; Teegavarapu and Chandramouli, 2005). The most common methods are based on averaging nearby hard data points. Other methods are based on minimizing the roughness of the interpolated property (e.g. splines; Ahlberg et al., 1967; Dubrule, 1984; Mitasova and Mitas, 1993, Mitasova and Hofierka, 1993) or in polynomial fitting; these methods are not as flexible, realistic and exact as average-based methods and therefore will not be discussed further here. Average-based methods differ on the procedure to obtain the weights for each nearby hard data point; two widely used approaches are introduced here: a) inverse distance weighting, and b) kriging.

a) Inverse distance weighting is a simple set of methods, in which the weights for each averaged hard data point are assigned based on an inverse of distance criterion (Kane et al., 1982; Pebesma and Wesseling, 1998). Usually, the inverse of the squared distance is used, as in the example presented here. Soft data needed in inverse distance weighting corresponded to the geometric anisotropy factor (Kupfersberger and Deutsch, 1999). This factor is used to multiply the vertical coordinates before the estimation (Jones et al., 1986; Zoraster, 1996). This enables assigning different weights to hard data points located at the same real distance from the point being estimated, but with differing stratigraphic position, and allows reproducing flattened geometries, which are typical of sedimentary deposits. In order to obtain objective measures of the anisotropy factor, this was derived from the anisotropy measured by variogram ranges (see below), and was set to the ratio between horizontal and vertical variogram range (Table 1).

b) Kriging is a geostatistical method in which the weights for each averaged hard data point are defined to minimise the estimation variance (Matheron, 1963; Journel and Huijbregts, 1978; Cressie, 1990). The minimisation of the estimation variance enables a spatial covariance criterion to be introduced, which results in weights for each data point that not only depend on the distance and direction to the grid cell being estimated (as in inverse distance weighting), but also on the characteristics of the interpolated property (described by the variogram, see below) and the relative positions of the averaged hard data (redundancy factor). This fact makes kriging estimates more robust than the results yielded by inverse distance weighting methods (e.g. Falivene et al., 2007), especially in cases where hard data are not located following a regular pattern. Soft data in kriging include variograms, which are a measure of the degree of correlation of a property as a function of distance (Journel and Huijberts, 1978; Isaaks and Srivastava, 1989; Gringarten and Deutsch, 2001). Variogram parameters (shape of the variogram, nested structures, sill contributions and horizontal and vertical ranges; Deutsch and Journel, 1998) were derived from the values assigned to hard data (Table 1). Apart from the estimated grid cell value, kriging also provides the estimation variance (Journel, 1986); this is a measure of the reliability of the estimated value, which depends on the data configuration and on the variogram of the property. The estimation variance is not directly used in interpolation algorithms, but is crucial for truncated gaussian simulation method (see stochastic facies modelling methods section).

TABLE 1 **Soft data parameters for continuous methods (TIDW and TK) applied to obtain deterministic facies reconstructions of the As Pontes basin dataset.**

Anisotropy Factor	228			
	Sill contribution	Theoretical variogram model	Horizontal Range (m)	Vertical Range (m)
Variogram	0.6	Exponential	500	1.4
	0.4	Exponential	100	3.0

The final step of continuous methods is to truncate the interpolated transformed property with the thresholds between facies categories (Fig. 8). This allows the facies reconstructions to be obtained: truncated inverse distance weighting (TIDW; Fig. 9A), and truncated kriging (TK; Fig. 9B). The algorithm implementation for TIDW was based on the inverse squared distance weighting implementation in the GSTAT software package (Pebesma and Wesseling, 1998), whereas TK used the kriging code available in GSLIB (Deutsch and Journel, 1998).

Indicator Kriging and Indicator Inverse Distance Weighting (categorical methods)

Preliminary data transformations

The first step in categorical methods for facies reconstruction (Fig. 5) is the indicator transformation (Journel, 1983; Gómez-Hernández and Srivastava, 1990) of facies categories. The indicator transformation applied to categorical variables like facies, transforms each facies into a new variable, called an indicator. The value of these new variables corresponds to the probability of finding the related facies at a specific position. Where hard data exist, the value of the indicator variable corresponding to the facies present is set to one, whereas the values of all the other indicator are set to zero.

Interpolation algorithm and results

The following step in facies reconstruction using categorical methods is to interpolate each new indicator variable at each grid node. Either inverse squared distance weighting and kriging (see above) were used. Soft data parameters describing each new indicator facies-related variable (anisotropy factors for IIDW and variograms for IK) were extracted from the transformed hard data (Table 2).

TABLE 2 | **Soft data parameters for categorical methods (IIDW and IK) applied to obtain deterministic facies reconstructions of the As Pontes basin dataset.**

Anisotropy Factors	LM Facies	228			
	PBC Facies	99			
	DBC Facies	228			
	XBC Facies	142			
	AM Facies	113			
		Sill contribution	Theoretical variogram model	Horizontal Range (m)	Vertical Range (m)
Variograms	LM Facies	0.018	Exponential	500	1.4
		0.012	Exponential	100	3.0
	PBC Facies	0.063	Exponential	200	1.4
		0.042	Exponential	100	3.0
	DBC Facies	0.150	Exponential	500	1.4
		0.100	Exponential	100	3.0
	XBC Facies	0.039	Exponential	300	1.4
		0.026	Exponential	100	3.0
	AM Facies	0.113	Exponential	700	1.4
		0.076	Exponential	100	3.0

By assembling the interpolation results obtained for all the indicator variables, the facies occurrence PDF at each grid node is determined. The probability of finding each facies varies from 1 (full probability) to 0 (null probability). The facies with the highest probability at each grid node is selected as the one present at that node, enabling to obtain the facies reconstructions: indicator inverse distance weighting (IIDW; Fig. 9C), and indicator kriging, (IK; Fig. 9D). The algorithm implementation for IIDW was based the on inverse squared distance weighting implementation in the GSTAT software package (Pebesma and Wesseling, 1998), whereas IK used the kriging code available in GSLIB (Deutsch and Journel, 1998).

STOCHASTIC FACIES MODELLING METHODS

In order to illustrate stochastic FRM methods the results obtained from modeling the second dataset are used. This dataset derives from turbidite deposits in the Ainsa basin (NE Spain). Examples on the use of stochastic facies modelling methods in the literature will be introduced before presenting the application of the different methods to the Ainsa basin dataset.

Background on the use of stochastic facies modelling methods

A large number of published studies have used stochastic methods for facies modelling; some relevant applications in the literature are outlined below.

Pixel-based methods

Truncated Gaussian simulation (TGS; Galli et al., 1994; Journel and Ying, 2001) has been used to reproduce depositional settings assuming highly ordered depositional models, e.g. deltaic (Matheron et al., 1987; Rudikiewicz et al., 1990; Joseph et al., 1993), fluvial (Mathieu et al., 1993; Eschard et al., 1998), or turbiditic channel fills (Felletti, 2004). Two important variations of TGS have been developed (Fig. 5). One is the truncation of the sum of a Gaussian field and a deterministic expectation trend (MacDonald and Aasen, 1994), which reproduces ordered facies belts showing indentations between them (Fig. 10), and it has been used to model facies belts within deltaic depositional systems (MacDonald et al., 1992; MacDonald and Aasen, 1994; Jian et al., 2002; Castellini et al., 2003), and gradual facies transitions (Falivene et al., 2006c). The other is the truncation of plurigaussian fields, based on combinations of several sequential Gaussian simulations, which allows reproducing more complex spatial relationships between facies than the original TGS method (Le Loc'h and Galli, 1996; Dowd et al., 2003; Fig. 11). Another remarkable application of two-dimensional TGS has been used to describe the presence or absence of shale drapes at the bounding surfaces of sandy deltaic deposits or turbiditic channel bases (Novakovic et al., 2002; Li and White, 2003).

Sequential indicator simulation (SIS) has been applied in a variety of depositional settings assuming no facies ordering, such as fluvial (Langlais et al., 1993; Journel et al., 1998; Seifert and Jensen, 1999, 2000), deltaic (Cabello et al., 2007), aeolian (Sweet et al., 1996), and turbidite settings (Journel and Gómez-Hernández, 1993). A variation of SIS that accounts for transition probabilities has been developed (transition probability geostatistics, Fig. 5; Carle and Fogg, 1996, 1997). This variant is based on Markov chains (Gingerich, 1969; Harbaugh and Bonham-Carter, 1970), and defines facies transition probabilities as the probability for a facies to be present in a location, provided that another facies is present at another location. Facies transition probabilities are taken into account within the general SIS procedure at the time of computing the facies occurrence PDF. Applications of this variant have been used to model facies distribu-

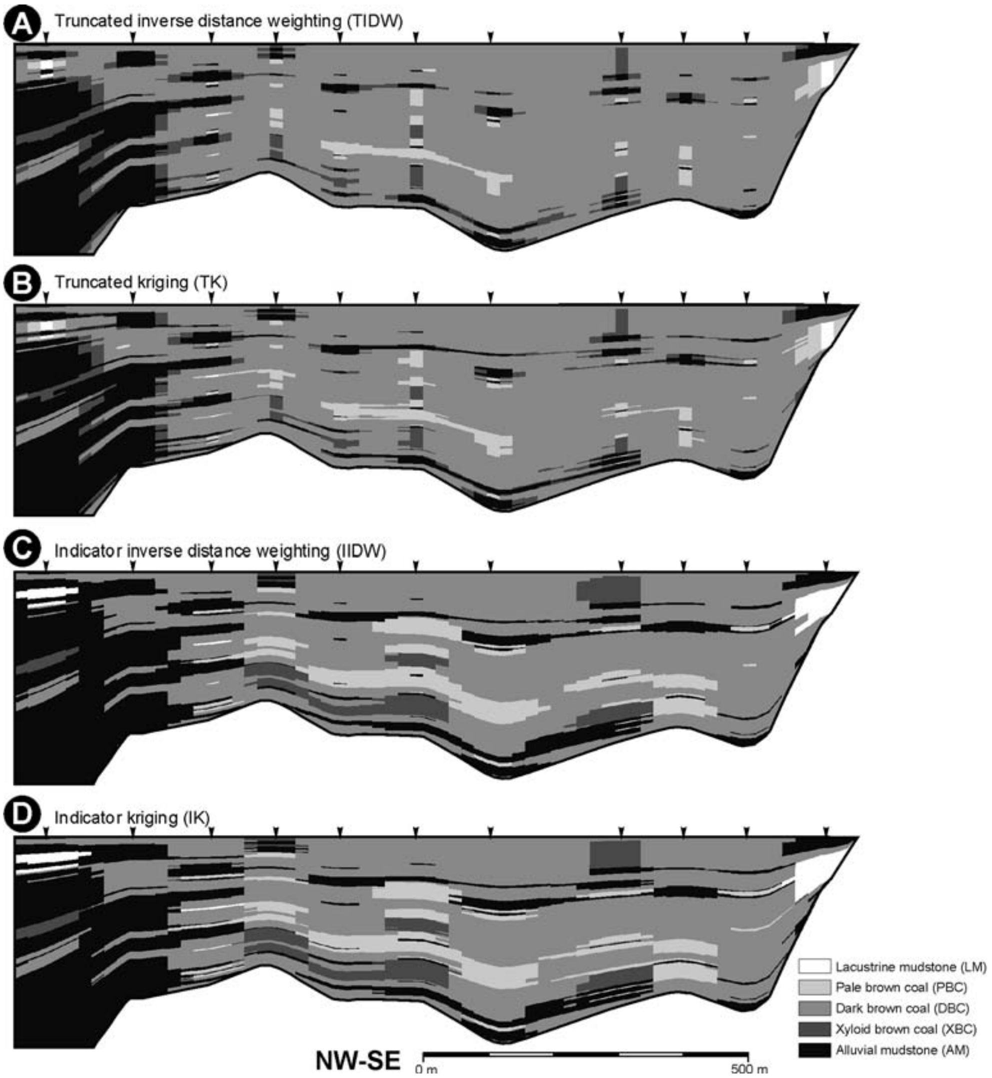

FIGURE 9 | **Section showing facies distributions derived from deterministic reconstruction methods applied to the As Pontes basin dataset. (A, B) were derived from continuous pixel-based methods, whereas (C, D) from categorical pixel-based methods. The position of the section is shown in Figure 7D. Arrows indicate the position of intersected wells (hard data). Vertical exaggeration is 10x.**

tion in alluvial fans (Fogg et al., 1998; Carle et al., 1998; Weissmann et al., 1999; Weissmann and Fogg, 1999; Weissmann et al., 2002; Fig. 12).

Multiple-point geostatistics (MPG: Guardiano and Srivastava, 1993; Wang, 1996; Caers, 2001; Strebelle, 2002; Caers and Zhang, 2004; Liu, 2006) is a more recent approach, developed to reproduce depositional conceptual models with well-defined shapes, in cases where conditioning to numerous hard data is needed (e.g. fractures, Wang 1996; or fluvial and turbidite channels, Strebelle and Journel, 2001; Strebelle et al., 2002; Caers and Zhang, 2004).

Object-based methods

The earliest applications of object-based methods focused on the simulation of horizontal and planar shales (Fig. 5), which could not be confidently correlated between neighbouring wells (Delhomme and Giannesini, 1979; Haldorsen and Chang, 1986; Haldorsen et al., 1987).

Object-based methods have also been successful in simulating channelized depositional systems (Fig. 5), because the external geometry of the related depositional elements (channel-belts, channels, crevasse channels or overbank deposits) can easily be parameterised as objects characterized by relatively simple shapes. Many different methods, the earliest ones aimed to improve the evaluation of hydrocarbon reserves in North Sea fluvial reservoirs, have been developed (Clementsen et al., 1990; Wadsley et al., 1990; Hirst et al., 1993; Tyler et al., 1994b; Hatloy, 1994; Deutsch and Wang, 1996; Holden et al., 1998; Viseur et al., 1998; Skorstad et al., 1999; Deutsch and Tran, 2002), with many successful applica-

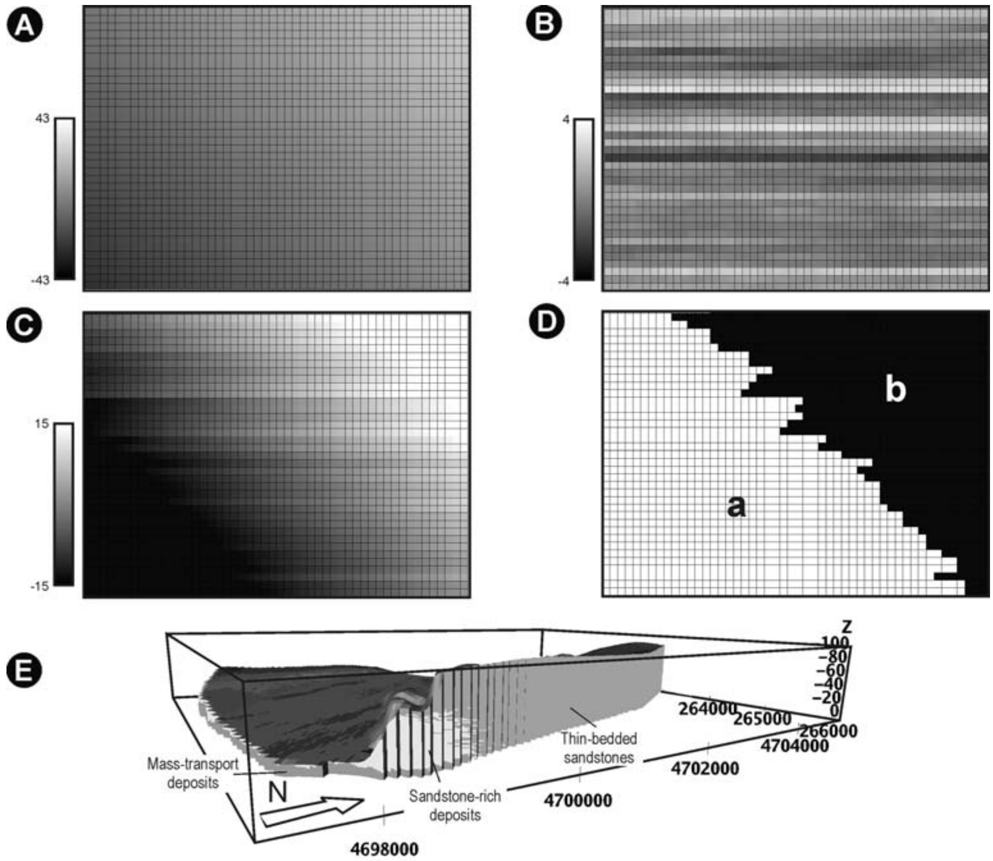

FIGURE 10 | **Illustration of the different stages to reproduce gradual facies transitions using a pixel-based stochastic modelling method based on the truncation of the sum of a deterministic expectation trend and a Gaussian field. A) Deterministec expectation trend. B) Gaussian field. C) Sum of the expectation trend and the Gaussian field. D) Truncation of the sum, obtaining two different facies units (a and b) with a gradual change between them. E) Application of this method to model gradual facies transitions within a turbidite channel-complex, paleocurrent is to the NW(simplified from Falivene et al., 2006c).**

tions (Stanley et al., 1990; Jones et al., 1995; Mijnssen, 1997; Journel et al., 1998; Seifert and Jensen, 2000). Object-based methods are also currently being applied to deep-water channelized deposits (Jones and Larue, 1997; Jones, 2001; Hodgetts et al., 2004; Larue and Friedman, 2005). An example of a facies distribution obtained using an object-based modelling method designed for reproducing channelized depositional systems is shown in Fig. 13.

More generic object-based methods have also been developed (Gundeso and Egeland, 1990; MacDonald and Halland, 1993; Lia et al., 1996), like Ellipsim (Deutsch and Journel, 1998) or the advanced object-based method presented and used for modelling the Ainsa basin dataset (see below). These are based on introducing objects of a certain shape, in most cases ellipses or parallelepipeds.

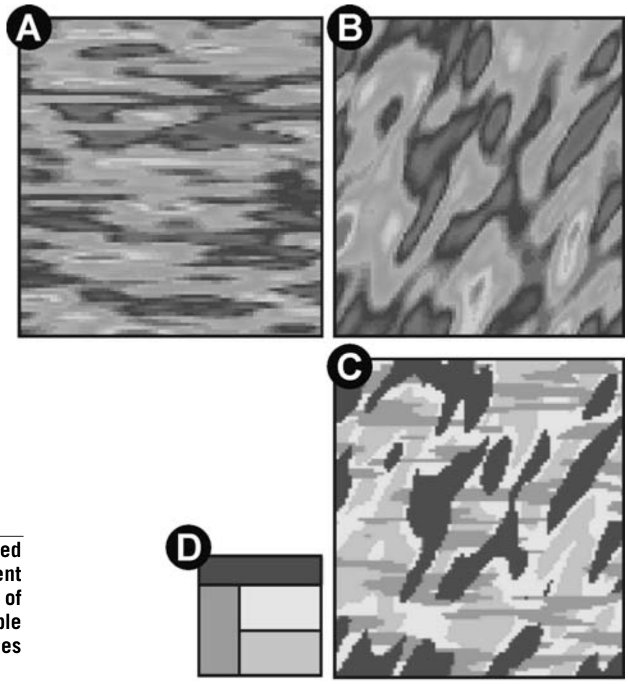

FIGURE 11 | **Illustration of the pixel-based stochastic modelling method based on the truncation of plurigaussian fields. A, B) are images of two different Gaussian fields. C) Facies model derived from the combination and truncation of the two Gaussian fields. D) Graphical plot showing the rules related to permissible facies transitions used to combine the Gaussian fields and generate the facies model. Simplified from Beucher et al. (2003).**

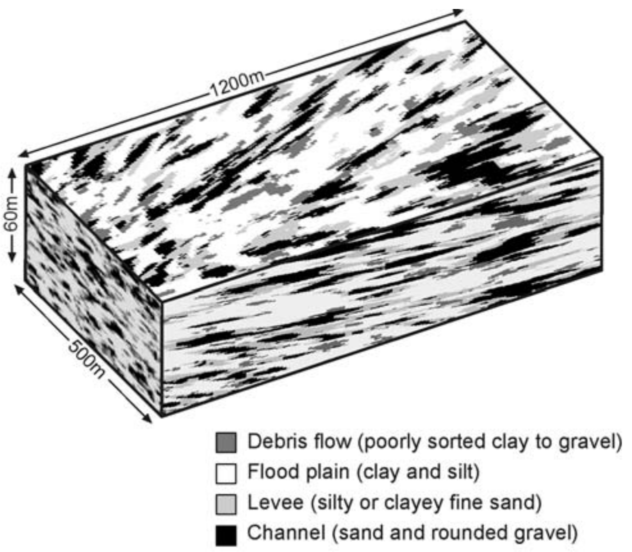

FIGURE 12 | **Three-dimensional facies simulation showing the architecture of alluvial fan deposits obtained by using transition probability geostatistics. Note the reproduction of fining-upward (channel to levee) tendencies, which cannot be simulated with traditional sequential indicator simulation (SIS). Simplified from Carle et al. (1998).**

The most advanced general object-based methods can approach a variety of conceptual depositional models by changing the object geometries (shape, roughness, undulations), parameters (orientation, dimensions, correlation factors between dimensions), and their relationships (repulsion factors, varying proportions along grid zones) (Brandsaeter et al., 2001; Cunha et al., 2001; Purvis et al., 2002; Smith and Møller, 2003; Conybeare et al., 2004; Pringle et al., 2004; Satur et al., 2005; Falivene et al., 2006c).

Application of facies modelling methods to the Ainsa basin dataset

Introduction

The Ainsa basin is the slope portion of a Lower Eocene foredeep, which developed in the footwall of the western oblique ramp of the Montsec thrust sheet (Fig. 14A; Muñoz, 1998; Fernández, 2004; Fernández et al., 2004). The slope complex is mostly made up of mudstones with a number of embedded sandy and conglomeratic turbidite systems; among which the Ainsa turbidite system (Mutti, 1985; Mutti et al., 1988; Arbués et al., 1998; Fernández et al., 2004). The information used herein is derived from the so-called Quarry outcrop (Figs. 14B and C), where the basal part of the lowermost cycle of channel-complex development and abandonment of the Ainsa turbidite system is exposed (Arbués et al., in press). Mutti and Normark (1987), Schuppers (1993, 1995), Clark and Pickering (1996) and Arbués et al. (in press) have presented sedimentological descriptions and interpretations for this outcrop. Only the information related to the sandstone-rich, turbidite-filled, C2 interval in the detailed characterization by Arbués et al. (in press) was used for this study (Fig. 14C). The exposed section of interval C2 is nearly 30 m thick and 750 m long, and oriented oblique (SSE-NNW) to the paleoflow direction (WNW).

Given the relatively high degree of heterogeneity present in the facies distribution and the availability of a detailed outcrop characterization (Fig. 14C), this dataset was deemed useful to illustrate the results obtained by stochastic modelling methods (Fig. 5). The objective of these methods is to generate facies distributions resembling the spatial patterns observed at the outcrop. Continuous methods (TGS), categorical methods (SIS and MPG), and object-based methods (Ellipsim and an advanced general object-based method) were applied.

Another widely used stochastic modelling methods were introduced above (e.g. truncation of the sum of an expectation trend and a Gaussian field: Fig. 10; truncation of plurigaussian fields: Fig. 11; transition probability geostatistics: Fig. 12; object-based methods reproducing horizontal and planar shales; and object-based methods reproducing channelized depositional systems: Fig. 13); but these were not applied to the Ainsa dataset because they are considered unsuitable for reproducing the sedimentary heterogeneity observed in the Quarry outcrop (Fig. 14C).

General set up

The outcrop characterization used as the starting point for application of stochastic modelling methods (Fig. 14C) was constructed from a photomosaic and a number of closely spaced stratigraphic logs. A widespread shale layer located in the middle of the C2 interval was used as

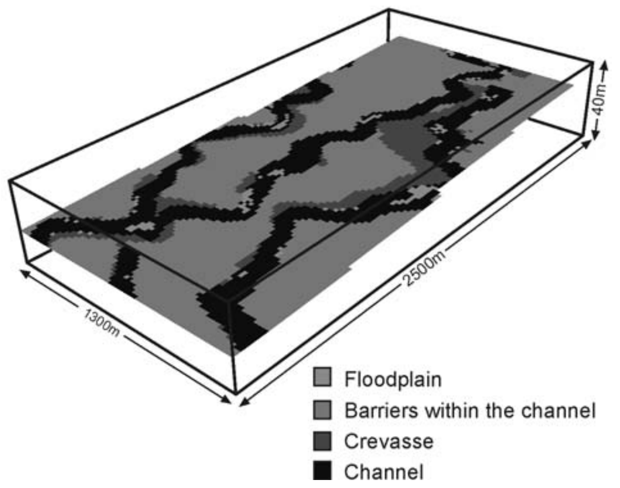

FIGURE 13 | **Horizontal section showing facies architecture from a three-dimensional model obtained by using a stochastic object-based modelling method designed to reproduce channelized depositional systems.**

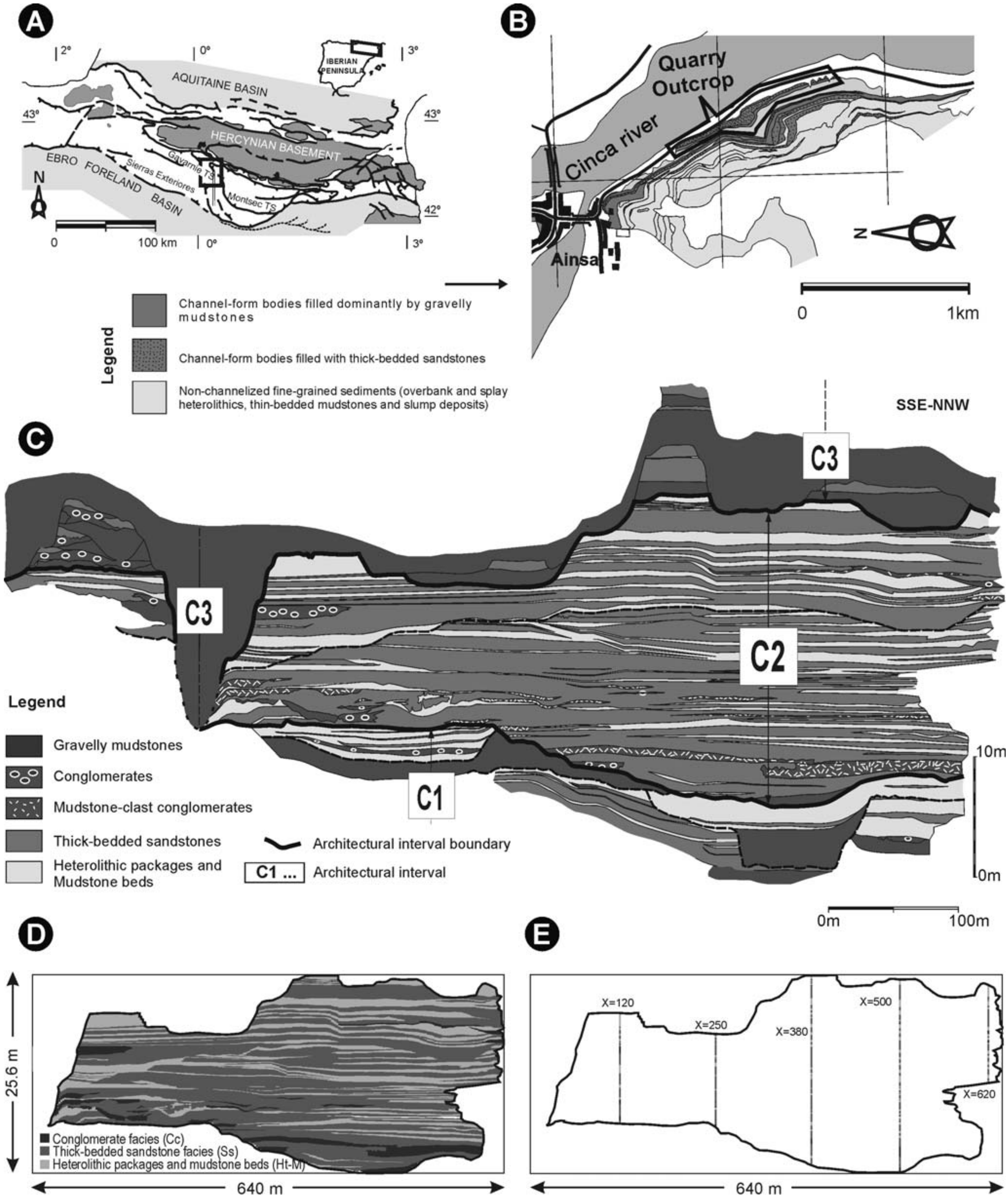

FIGURE 14 **A) Location of the Ainsa basin (boxed area) within the Pyrenean context. B) Geological map of the Quarry outcrop and surrounding areas (simplified from Arbués et al., in press). C) Sedimentological characterization of the Quarry outcrop (simplified from Arbués et al, in press). D) Gridded and simplified characterization corresponding only to the C2 architectural interval. E) Hard data used to condition the facies models.**

datum to correlate the logs (Fig. 14C); this allowed us to consider the general bedding in C2 as parallel to the horizontal for facies modelling purposes. The C2 interval in the characterization was resampled onto a 2D rectangular grid with cells oriented parallel to the horizontal datum (Fig. 14D). Cell dimensions were 2.5 m wide and 0.05 m high; the modelling grid used the same layering style and spacing. Only three facies were considered for modelling purposes: thick-bedded sandstones (Ss), conglomerates (Cc) and heterolithic packages and mudstone beds (Ht-M).

Hard data consisted of five, regularly spaced, vertical logs extracted from the gridded characterization (Fig. 14E). Hard data were not dense enough to allow the accurate extraction of some soft data parameters; instead, these were derived from the gridded outcrop characterization (Fig. 14D). Soft data included facies proportions (7% for Cc, 63% for Ss and 30% for Ht-M; Fig. 15), variograms (Table 3), indicator variograms (Table 4), object parameters (Table 5), and indirectly, training images (Fig. 16).

Truncated Gaussian Simulation (continuous methods)

Preliminary data transformations

The first step in pixel-based, continuous methods for facies modelling (Fig. 5) is the transformation of facies categories into a continuous property, as in continuous

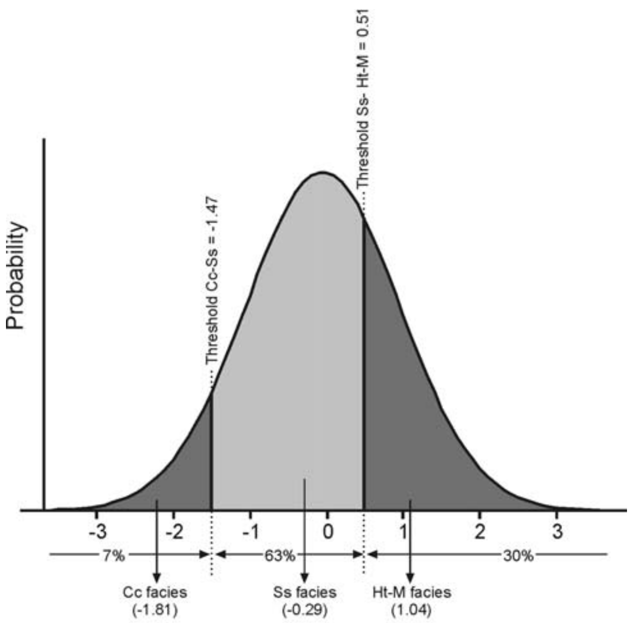

FIGURE 15 **Illustration of the transformation of facies categories to a continuous variable assuming a Gaussian distribution for the Ainsa dataset. Note the proportions of each facies, the thresholds between facies categories, and the values of the continuous property assigned to each facies in brackets. Cc stands for conglomerates, Ss for sandstones, and Ht-M for heterolithics and mudstones.**

deterministic facies reconstruction methods (Fig. 8). This requires an ordering of facies based on the conceptual depositional model. In the Ainsa dataset facies were ordered following grain-size and energy-related paleoenvironment criteria (Cc, Ss and Ht-M; Fig. 15). Continuous methods start by calculating the thresholds between facies; assuming a Gaussian distribution, the areas between thresholds correspond to the measured proportions in the hard data (Fig. 15). The next step is to assign to each facies a value between their thresholds; constant values located in the centre of each category were used (Fig. 15; Deutsch, 2002). Variogram parameters were derived from the outcrop characterization transformed into a continuous property (Table 3).

Simulation algorithm and results

The second step consists of building a simulated random field of the transformed continuous property extending all over the modelling grid. This field is conditioned by the hard data (Fig. 14E) and reproduces the previously computed variograms, which characterize the spatial variability of the continuous property (Table 3). Several algorithms have been designed for building simulated fields, among these those based on the turning bands (Matheron, 1973; Journel, 1974; Tompson et al., 1989), post-processing with simulated annealing (Deutsch and Cockerham, 1994), lower-upper Cholesky decomposition (Alabert, 1987; Davis, 1987) or sequential Gaussian simulation (Deutsch and Journel, 1998). Sequential Gaussian simulation has proven to be the most powerful and straightforward algorithm (Koltermann and Gorelick, 1996; Deutsch and Journel, 1998), and is currently the most widely used. Therefore only this algorithm will be discussed herein. Sequential Gaussian simulation (Deutsch and Journel, 1998; Journel and Deutsch, 1993) assigns a value to each grid cell sequentially, by following a preset path visiting all the modelling grid nodes. The assignation is made by random sampling from a PDF function, which is calculated for each grid node by assuming a Gaussian distribution described by the mean value and the standard deviation predicted by kriging interpolation (Cressie, 1990; see above). The kriging interpolation at each grid node is conditioned by hard data, previously simulated node values, and variograms. Sequential Gaussian simulation used the code provided in GSLIB (Deutsch and Journel, 1998).

TABLE 3 **Variogram parameters for continuous assumption methods (TGS) applied to obtain stochastic facies models of the Ainsa basin dataset.**

	Sill contribution	Theoretical variogram model	Horizontal Range (m)	Vertical Range (m)
Variogram	0.82	Exponential	120	0.6
	0.18	Exponential	1000	5.0

The final step of continuous methods is to truncate the simulated transformed property with the thresholds between facies categories (Fig 15). This yields the facies models: truncated Gaussian simulation (TGS; Fig. 17B).

Sequential Indicator Simulation (categorical methods)

Preliminary data transformations

Sequential indicator simulation (SIS) belongs to pixel-based categorical stochastic modelling methods (Fig. 5). This method is based on the indicator transformation (Journel, 1983; Journel and Alabert, 1989; Gómez-Hernández and Srivastava, 1990) of the facies categories (similar to categorical deterministic facies reconstruction methods). The indicator transformation applied to categorical variables like facies, transforms each facies into a new variable, and the value of each new variable corresponds to the probability of finding the related facies at a specific position. Where hard data exist, the value of the indicator variable corresponding to the facies present is set to one, whereas the values of all the other indicator variables are set to zero. Indicator variograms were derived from the indicator variables of the transformed outcrop characterization (Table 4).

Simulation algorithm and results

SIS assigns a facies value to each grid cell sequentially, by following a preset path visiting all the modelling grid nodes. SIS applied to categorical variables only differs from sequential Gaussian simulation in the procedure to compute the PDF. At each grid cell, the PDF in SIS is computed from the interpolated values derived from kriging of each indicator variable (i.e. the probability of finding each facies). Kriging of each new indicator variable in turn is conditioned by transformed hard data, previously simulated node values, and soft data (indicator variograms; Table 4). Kriging of each new indicator variable does not guarantee that the estimated probabilities for each facies are comprised between 0 and 1, and that the sum of the probabilities equals 1; verifying and correcting for these two properties should be performed in order to generate a permissible facies ocurrence PDF (Langlais et al., 1993; Deutsch, 2002), from which to sample the facies values. The simulated field obtained corresponds directly to the SIS results (Fig. 17C). The implementation of SIS provided in GSLIB (Deutsch and Journel, 1998) was used.

TABLE 4 | **Indicator variogram parameters for categorical assumption methods (SIS) applied to obtain stochastic facies models of the Ainsa basin dataset.**

		Sill contribution	Theoretical variogram model	Horizontal Range (m)	Vertical Range (m)
Variograms	**Cc Facies**	0.04	Exponential	112	0.75
		0.025	Exponential	500	2.5
	Ss Facies	0.23	Exponential	115	0.46
	Ht-MN Facies	0.16	Exponential	112	0.46
		0.05	Exponential	400	0.5

Multiple Point Geostatistics (categorical methods)

Simulation algorithm and results

Multiple point geostatistics (MPG; Guardiano and Srivastava, 1993; Wang, 1996; Caers, 2001; Strebelle, 2002; Caers and Zhang, 2004; Liu, 2006) belongs to the pixel-based categorical stochastic modelling methods (as SIS, Fig. 5). MPG does not require any preliminary data transformation. MPG assigns a facies value to each grid cell sequentially, by following a preset path visiting all the modelling grid nodes. The differences between MPG and SIS stems from the procedure to compute the facies ocurrence PDF at each grid cell. In MPG, like in SIS, the facies ocurrence PDF is computed by considering hard data, previously simulated nodes and soft data. However, in MPG the soft data considered are training images (Fig. 16), instead of indicator variograms. A training image is a template from which to find spatial configurations of facies resembling the one around the node to be simulated. The spatial configuration of facies around the node to be simulated is determined by considering neighbouring hard data and previously simulated nodes. Then, similar spatial configurations are searched for in the training image; from each of the spatial configurations found, the facies of the corresponding homologous node is recorded. The obtained facies records are used to construct the facies ocurrence PDF corresponding to the node being simulated.

The training image represents a conceptual image of the sedimentary heterogeneity to be reproduced in the simulated facies model. Training images have been generally derived from object-based realizations (Fig. 16; Strebelle, 2002; Caers and Zhang, 2004). Outcrop characterizations could also be used as training images; in the case of the Ainsa basin dataset this was not feasible, because the characterization width was not large enough to assure the reproduction of large-scale correlation patterns (Caers and Zhang, 2004). The resultant facies model obtained with MPG is shown in Fig. 17D. MPG used the SNESIM code (Strebelle, 2002).

Ellipsim and an advanced general object-based method (object-based methods)

Object-based methods are stochastic facies modelling methods. Among the many available object-based algo-

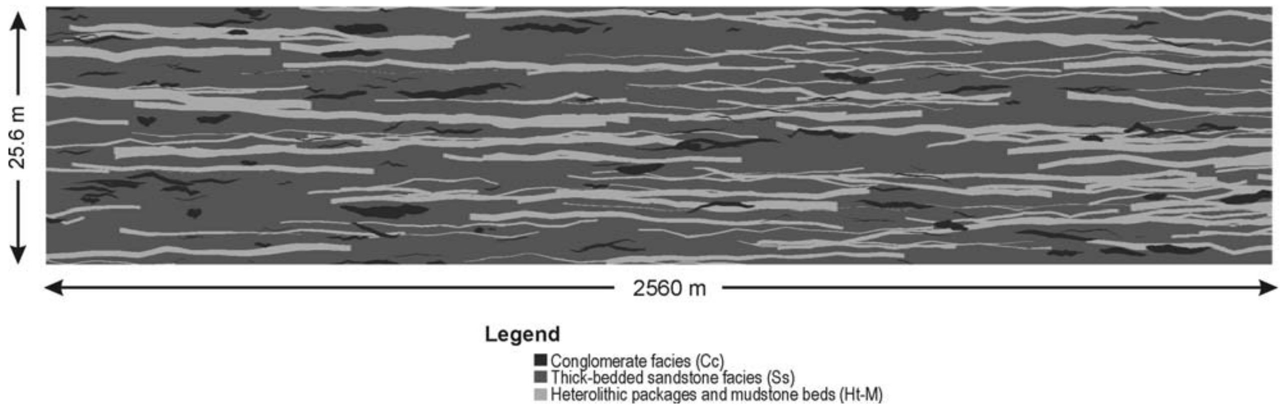

FIGURE 16 | **Training image used in multiple point geostatistics, applied to obtain stochastic models of the Ainsa basin dataset. The image corresponds to an unconditioned realization obtained with an advanced general object-based modelling method. Note the change of scale respect to Figures 14D and 17.**

rithms, we used two with different modelling capacity: Ellipsim and an advanced general object-based method (Fig. 5). In both cases, the Ss facies was used as background, since it is the most laterally extensive facies, into which objects of the Cc and Ht-M facies were introduced.

The Ellipsim method, coded by Deutsch and Journel (1998) is a very simple object-based algorithm, which only handles elliptical objects with constant orientation of their main axes, and is not capable of conditioning to hard data. It can only introduce objects of a unique facies in each run, therefore the modelling was split into three steps: 1) modelling of facies Ht-M in a background of facies Ss; 2) modelling of facies Cc in a background of facies Ss; and 3) merging the two realizations into a single one. The sedimetological criterion used for merging is that the Cc facies erodes/replaces the Ht-M and Ss facies; a resultant facies realization is shown in Fig. 17E. Soft data for Ellipsim consisted of geometric parameters characterizing the ellipses (proportions and dimensions), and were derived from the outcrop characterization (Table 5).

Concerning the advanced general object-based method, we refer to an algorithm able to reproduce complex geometries introduced by Lia et al. (1996), and implemented in the Irap RMS modelling package (by Roxar AS©; "Facies:Composite"). In addition to the basic set-ups for object-based facies modelling (different shapes, dimensions and correlation factors between dimensions), simulated Gaussian fields are used in this method to introduce undulations of the object centre plane and to add a degree of roughness to the top and base of each object, both giving the object shape a more realistic geometry. The simulation algorithm allowed conditioning to hard data, which is obtained with an iterative routine based on simulated annealing. The basic shape for the Cc elements was chosen as ellipses, aimed at reproducing their general lenticular external geometry. In addition, the parameters defining the centre plane and roughness were set to mimic the more detailed concave-convex nature of the erosive bounding surfaces observed on the outcrop. In the case of the Ht-M elements, rectangles were used as the basic shape, and undulations were set to a high degree, aimed at reflecting the overall geometry of these elements (Falivene et al., 2006a). Roughness was set at a low degree since small-scale erosive features are generally absent. Object dimensions were also derived from the outcrop characterization. A realization obtained using this method is shown in Fig. 17F.

TABLE 5 | **Object parameters for object-based methods (Ellipsim) applied to obtain stochastic facies models of the Ainsa basin dataset. Note that Ht-M proportions were increased to account for the erosion after merging with Cc facies. Three different types of Cc geometries were considered.**

		Percentage		Horizontal Radius (m))	Vertical radius (m)
Dimensions	Ht-M Facies	30%+2%		225	0.16
	Cc Facies	7%	5%	25	0.23
			5%	20	0.21
			90%	52	0.43

DISCUSSION AND CONCLUDING REMARKS

The first part of this section discusses critical issues that were encountered in the application of FRM methods to the studied datasets. Then, the capabilities and applicability of the methods are discussed by reference to the obtained results.

Critical issues in facies modelling

In order to obtain meaningful and reliable facies distributions with FRM methods, some important and critical

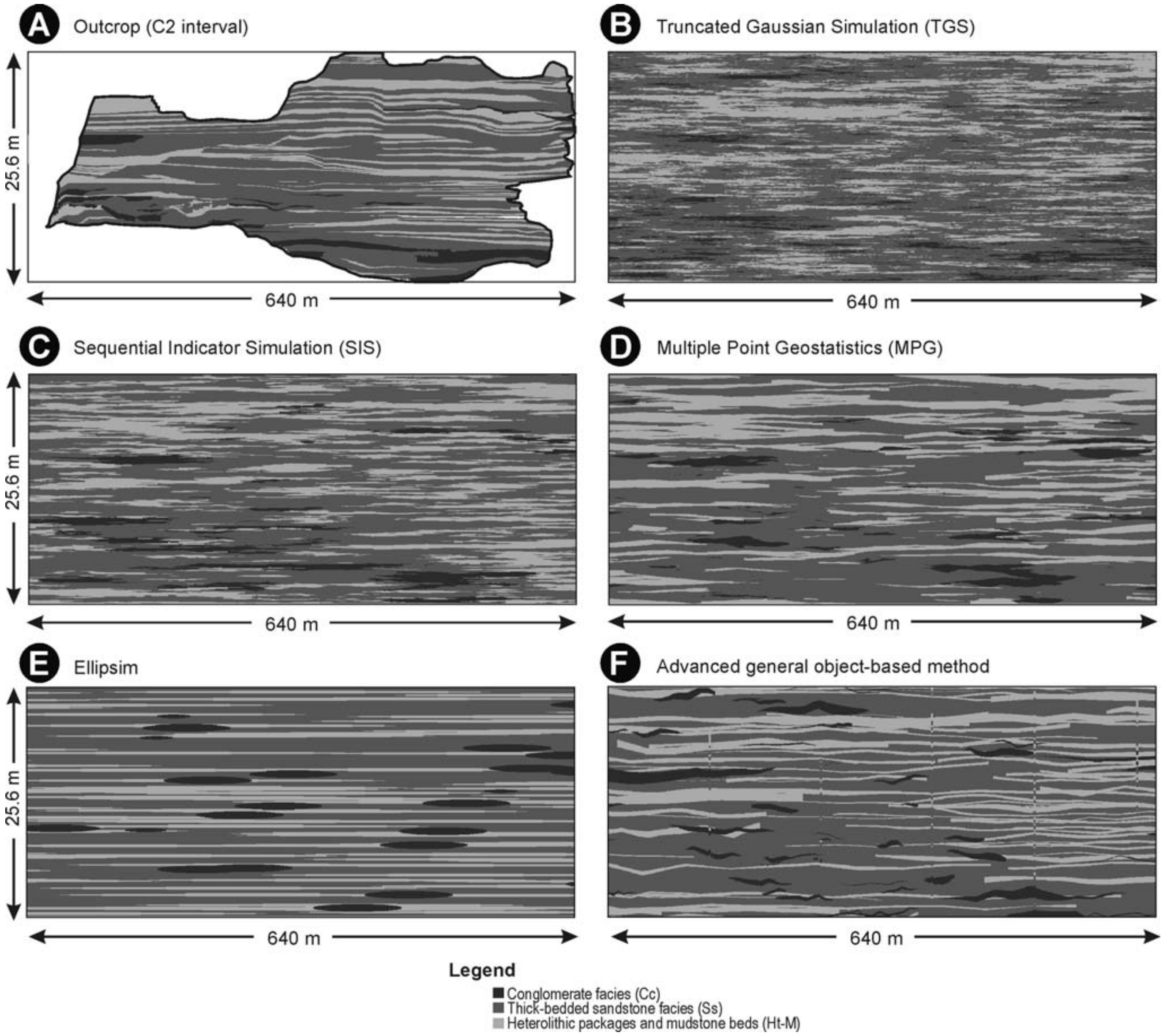

FIGURE 17 **A) Gridded and simplified characterization of the C2 interval. (B to F), Facies distributions derived from stochastic modelling methods, and trying to reproduce the sedimentary heterogeneity in frame A. Vertical exaggeration is 10x.**

issues linking input data and resultant facies distributions should be considered: a) stationarity and trends in proportions and geometrical characteristics of facies elements; b) reproduction of soft data in pixel-based methods; c) relationship between soft data parameters and resultant sizes of facies elements; and d) hard data conditioning.

Stationarity and trends

Pixel-based geostatistical methods (Fig. 5) were primarily designed for reproducing facies distributions that can be assumed stationary within the modelling grid (i.e. whose statistical properties, such as proportions, standard deviation and variograms, do not vary in space within the studied sedimentary body; Journel, 1985). However, facies distribution in the subsurface is usually affected by the presence of trends (i.e. facies proportions are not constant over the sedimentary body), these trends in most cases relate to variations in the depositional environment, either over different areas (horizontal trends) or over time (vertical trends).

When using deterministic methods in facies reconstruction (Fig. 5), and when hard data are relatively abundant, there are no significant differences between explicitly using a trend, which has been directly extracted from hard data, or not (Fig. 18). This is related to the fact that interpolation is done only with points located nearby, which implies that the search window is smaller than the trend wavelength and

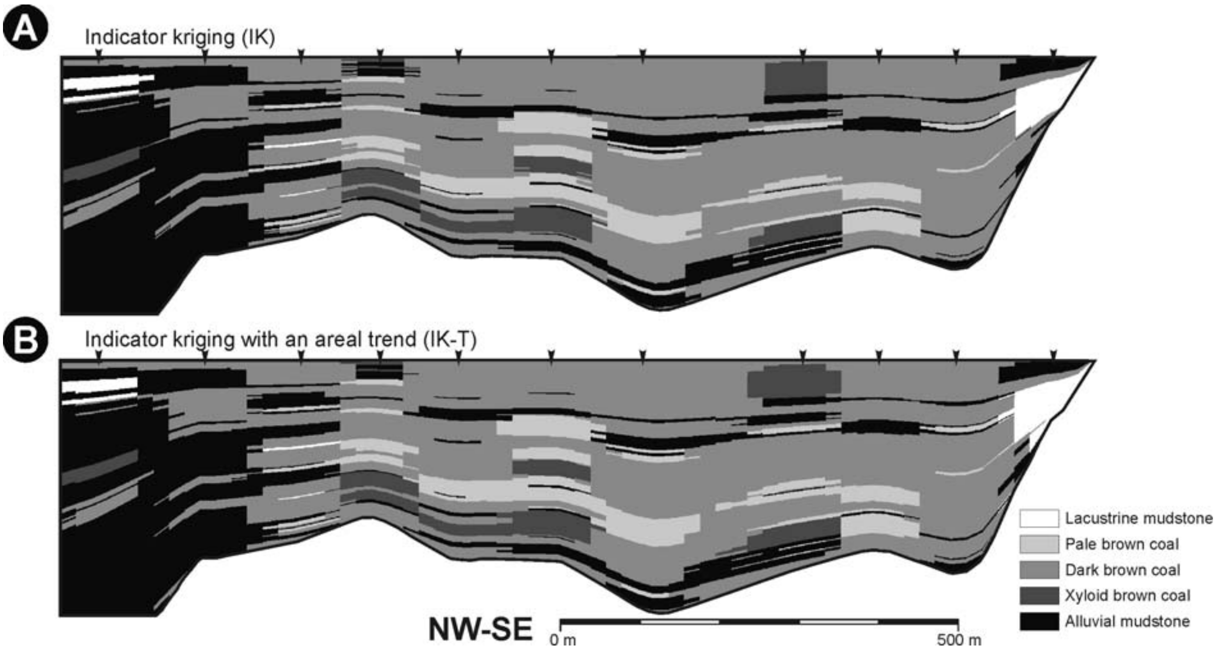

FIGURE 18 **Section showing facies distributions derived from deterministic reconstruction methods applied to the As Pontes basin dataset. A) was constructed by using indicator kriging, and B) by indicator kriging with an areal trend. The areal trend was extracted from the available hard data (i.e. wells) information (Figure 7D). Note the similarities of the resultant facies distribution, independently of whether a method considering areal trends explicitly is used or not. See Falivene et al. (2007) for detailed discussion. Position of the section is shown in Figure 7D. Arrows indicate the position of intersected wells (hard data). Vertical exaggeration is 10x.**

thus accounts implicitly for the modelled trend (Journel and Rossi, 1989; Falivene et al., 2007).

In contrast, when using stochastic methods for facies modelling (Fig. 5), trends are very important to reproduce a conceptual depositional model, as the simulation results are usually not heavily constrained by hard data. In most cases trends must be predefined derived from general geological knowledge or additional input data (e.g. geophysical information), depending upon the modelling method there are several ways to introduce them: a) trends in TGS can be accounted for by varying the truncation thresholds along the modelling grid (Galli et al., 1994; Mathieu et al., 1993); if strong trends are used the results obtained can be similar to those obtained using the method based on the truncation of the sum of an expectation trend and a Gaussian field (Figs. 5 and 10; MacDonald and Aasen, 1994); b) trends in TGS, SIS and MPG can be accounted for by introducing a term in the PDF related to the varying facies proportions (Langlais et al., 1993); and c) trends in object-based methods can be accounted for by varying the probabilities of object insertion depending upon the location in the grid (Lia et al., 1996; Falivene et al., 2006d).

Reproduction of soft data in pixel-based methods

When deterministic methods are used, input soft data (variograms and proportions) are not reproduced in the facies reconstruction. This is inherent to the interpolation approximation and relates to the smoothing effect of interpolation methods (Journel and Huijberts, 1978, p. 451; Isaaks and Srivastava, 1989, p. 268; Olea and Pawlowsky, 1996; Journel et al., 2000). See Falivene et al. (2007) for further discussion related to the quantification of the smoothing effect in the As Pontes basin reconstructions introduced herein (Fig. 9).

Oppositely, the objective of stochastic facies modelling is to reproduce soft data in the resultant facies model. However, if the modelling grid size is not large enough compared to the pixel-based typical soft data (i.e. variogram ranges or training images size); realizations showing smaller spatial continuity may result. Several procedures may help to alleviate this problem: a) Optimising the path visiting all the modelling grid nodes to improve the honouring of soft data (Tran, 1994); b) Performing simulations in larger grids and then cropping the area of interest, as it was done for TGS, SIS and MPG methods applied to the Ainsa basin dataset (Fig. 17B, C and D; Falivene et al., 2006a), and demonstrated in Fig. 19; and c) By using post-processing with simulated annealing (i.e. randomly changing simulated node values in order to minimize an objective function, which accounts for the reproduction of soft data in the resultant facies model; Goovaerts, 1996).

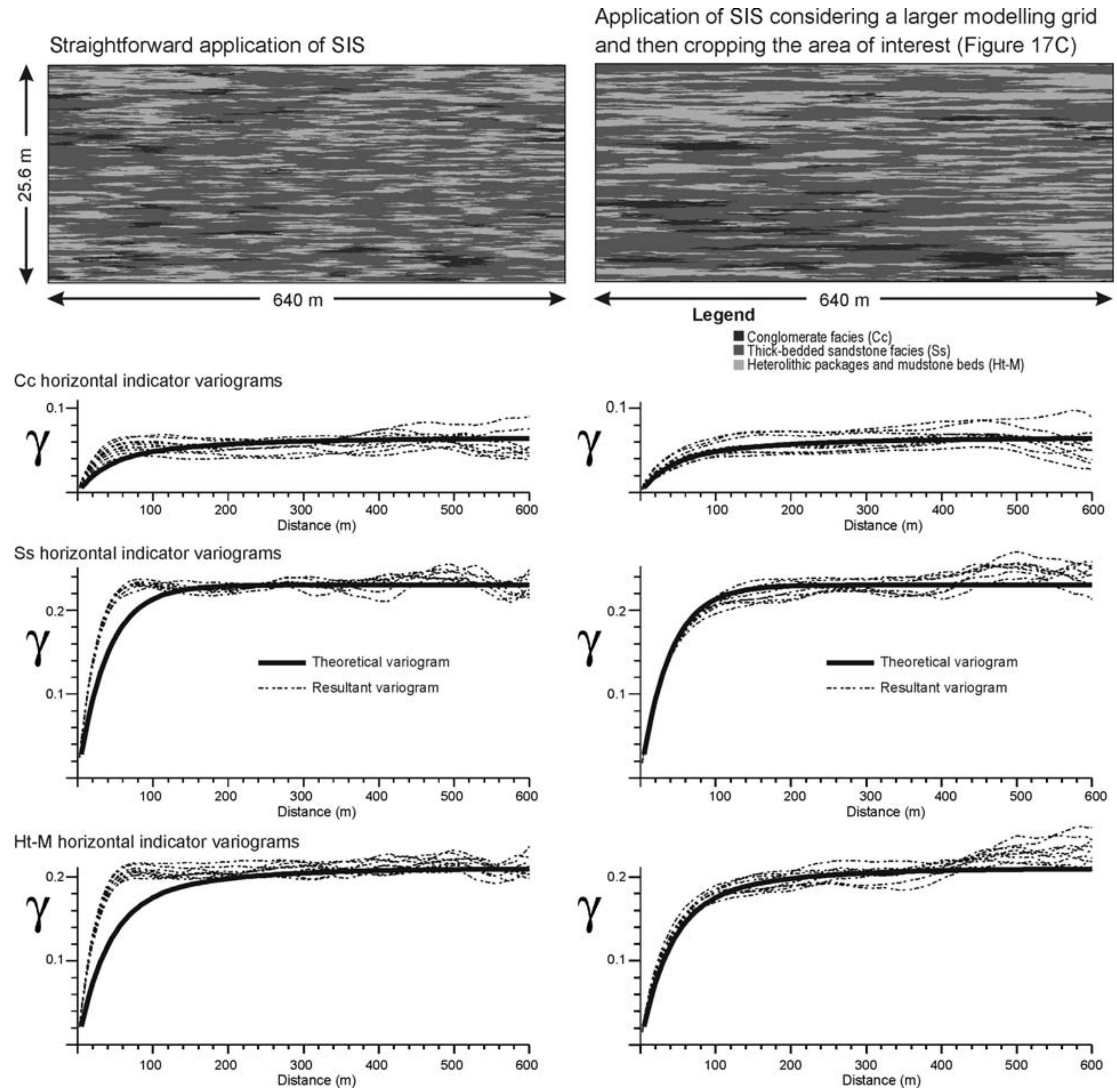

FIGURE 19 **Reproduction of soft data (i.e. variograms) in Sequential Indicator Simulation (SIS, Figure 5). The upper frames correspond to SIS realizations trying to reproduce sedimentary heterogeneity in Figure 17A. The left one was obtained through the straightforward application of SIS. The right one was obtained using a simulation area extending well beyond the grid limits (at least 20 times the variogram ranges), which was cropped to obtain the final facies model. The lower frames show the theoretical horizontal indicator variograms used in the simulations (continuous bold lines), and measured resultant horizontal variograms computed from different realizations (dashed lines). Note the improvement on theoretical variogram reproduction when a large simulation area is used (variograms on the right), respect to the straightforward application of SIS (variograms on the left).**

Relationships between soft data parameters and resultant sizes of facies units

Another important issue related to the application of FRM methods is the relationship between soft data parameters (i.e. variograms or training images) used to condition the modelling algorithm, and geometrical parameters describing the facies distribution (i.e. size of clustered values with the same facies, which are related to the sizes of facies units or elements that can be measured in outcropping analogues, and used in object-based modelling methods).

The sizes obtained with deterministic reconstruction methods (TIDW, TK, IIDW, IK; Fig. 5) are mostly controlled by the hard data (Fig. 9); and therefore, there is no straightforward link with the soft data parameters employed by these algorithms.

In SIS and TGS (Fig. 5), the relationship between modelling input parameters and sizes of output clustered values with the same facies is important. This relationship makes possible to relate the variograms, which are complex and may be difficult to infer, to easily quantifiable and intuitive parameters such as sizes. Moreover, it also allows the use of prior knowledge of the depositional system in order to define variograms. This relationship has been sometimes erroneously identified as controlled only by the variogram range. However, in SIS the resultant sizes are controlled by the slope of the variogram at the origin and the facies proportion (Carle and Fogg, 1996; Ritzi, 2000, Guardiola-Albert and Gómez-Hernández, 2001). Whereas in TGS and related methods (Fig. 5, 10 and 11) the controlling factors are more complex, as the grid spacing also exerts some influence (Guardiola-Albert and Gómez-Hernández, 2001). In MPG (Fig. 5), the sizes depend directly on the characteristics of the training image (Strebelle, 2002; Liu, 2006).

In object-based methods (Fig. 5), the relationship between object sizes specified as soft data and the resultant sizes of the elements in the facies model is straightforward and fully controlled by the modelling algorithm.

Hard data conditioning

Hard data conditioning in pixel-based methods (either deterministic or stochastic; Fig. 5) is achieved directly without approximations or iterations. On the other hand, conditioning to hard data in object-based models can be problematic in some cases. Object-based modelling methods condition facies observations following two main approaches. a) The simplest one is based on first placing those objects intersected by hard data information and later distributing non-intersected objects at random locations until the desired proportions are met (Clementsen et al., 1990; Gundeso and Egeland, 1990); and b) The more complex, flexible and time-consuming option is based on simulated annealing. Simulated annealing computes an objective function measuring the discrepancy of the model with respect to the selected conditions (soft data and hard data), propose a change to the seed model (e.g. moving or changing the characteristics of an object), and accept or reject this change depending upon the objective function evaluation improvement (Lia et al., 1996; Holden et al., 1998; Skorstad et al., 1999; Deutsch and Tran, 2002). In both approaches hard data conditioning may not be completely feasible, especially when a large number of soft data constraints are used, with a dense set of conditioning hard data observations that should be honoured compared to the object sizes. These facts may cause the modelling method to fail or not fully converge in a reasonable computing time (i.e. resulting in some non-realistic discontinuities near hard-data, e.g. Fig. 17F).

Methods applicability

The application of several FRM methods to generate facies distributions from two different datasets, such as the As Pontes basin and the Ainsa basin datasets, made it possible to illustrate and discuss on the applicability of a wide variety of reconstruction and modelling techniques.

Continuous versus categorical methods

Both deterministic and stochastic pixel-based continuous methods (Fig. 5) involve the simplification of facies categories to a single variable (Figs. 8 and 15). This simplification limits these methods by imposing two fundamental restrictions: a) continuous facies ordering. For examples see Figs. 9A and 9B, where a transitional step with facies XBC occurs in most transitions from AM to DBC. See also Fig. 17B, where a transitional step with facies Ss occurs in transitions from Cc to Ht-M, except in some rare very rapid changes along the vertical. The extreme case of an ordered facies distribution corresponds to the reproduction of interfingered transitions by the method based on the truncation of the sum of an expectation trend and a Gaussian field (Fig. 10); and b) the use of a single set of soft data parameters (one anisotropy factor in TIDW or one variogram model in TK or SGT; Tables 1 and 3) to constrain the spatial variability of facies distribution (de Marsily et al., 1998).

However, the simplification of facies categories to a single variable gives to continuous pixel-based methods their major advantages. 1) Relatively limited information or hard data are required to derive soft data parameters, and 2) continuous pixel-based methods are faster in terms of computing time than their equivalent categorical methods.

In contrast to continuous pixel-based methods, for categorical pixel-based methods all the facies transitions are possible (Figs. 9C and D, Figs. 17C to F) and each facies is characterized by one set of soft data parameters (Tables 2, 4 and 5). Categorical pixel-based methods are more suitable for generating facies distributions of general depositional models (Fig. 5); although they require more information to derive all sets of soft data and are more time consuming than the continuous methods. Continuous methods are only useful in depositional settings where it is reasonable to assume a highly ordered facies distribution (Fig. 5).

The truncation of plurigaussian fields (Fig. 11) and transition probability geostatistics (Fig. 12) represent approaches between continuous and categorical pixel-based methods that make it possible to obtain intermediate facies ordering results. In the case of object-based methods, the facies ordering would depend on the type of model that is chosen and particularly if repulsion factors between facies are used.

Deterministic versus stochastic methods

Deterministic methods were able to provide interpolation-based results, predicting the overall facies distribution patterns, from the hard data in the As Pontes basin dataset (Figs. 9 and 18). Stochastic methods were able to generate facies distributions reproducing the heterogeneity in the Ainsa basin dataset (Fig. 17). Deterministic methods provide a unique solution, whereas stochastic methods provide multiple equiprobable realizations, which can be used for quantifying uncertainty and in further non-linear post-processing, such as flow simulation (Falivene et al., 2006a).

The results of deterministic methods applied to facies reconstruction are controlled mainly by hard data. Considering that at least reasonable soft data parameters are used, the facies distributions obtained with the different interpolation algorithms (e.g. kriging or inverse distance weighting) are very similar for each assumption (for continuous methods compare Figs. 9A and B, and for categorical methods compare Figs. 9C and D; Falivene et al., 2007). Therefore the results are not extremely sensitive to the interpolation method, and the main difference comes from selecting a continuous method or a categorical method (Fig. 5). Categorical methods tend to provide facies distributions with lower smoothing effect (Falivene et al., 2007), and are thus preferred unless the facies ordering is really obvious. Markov analysis can be used to detect continuous facies ordering in hard data (Gingerich, 1969; Miall, 1973).

In contrast, the results of stochastic methods applied to facies modelling are mainly controlled by the mathematical approximations of the modelling method and the soft data parameters (Dubrule, 1994; Jones et al., 1995; Mijnssen, 1997). Results of the different methods may differ significantly; even when using soft data derived from the same dataset (Figs. 17B to F). The method chosen should be able to reproduce the depositional conceptual model at the scale of the problem (Journel et al., 1998; Figs. 5 and 17) and integrate all the available hard and soft data.

For modelling the Ainsa dataset, the selection of the method reproducing best the facies distribution observed in the outcrop would be dependent on the further use of the facies model; if this facies model were to be used for predicting flow-related responses, then the preferred modelling method would be the advanced general object-based method (Fig. 17F; Falivene et al., 2006a). However, there are no unequivocal rules for selecting the appropriate methods in each specific case, as this will depend on several factors: 1) the scale of the problem, 2) the type and density of data available, 3) the depositional setting, and 4) the objective of the model. Using the FRM methods presented herein, one should be able to model a wide range of settings. In complex situations, with heterogeneities in facies distribution occurring at different scales, it might be also useful to combine several methods in order to reproduce a given depositional conceptual model; such approaches are termed hierarchical (Mac Donald et al., 1992; MacDonald and Halland, 1993; Tyler et al., 1994a; Jones et al., 1995; Deutsch and Wang, 1996; Cunha et al., 2001; Deutsch and Tran, 2002; Falivene et al., 2006c).

Conclusions

The use of a surface-based framework, in combination with statistical grid-based facies reconstruction and modelling methods (FRM methods), provides a flexible and powerful approach to generating subsurface facies distributions constrained by a variety of input geological data.

The wide spectrum of existing FRM methods makes it difficult to choose the most appropriate method for a given studied case. Some basic rules for choosing between the different available methods have been stated with the application of FRM methods to the two selected datasets from the As Pontes and Ainsa basins:

1) Choosing between a deterministic facies reconstruction method and a stochastic facies modelling method would depend on the objective of the resulting facies distribution. On the one hand, if the aim is to capture the general facies distribution patterns then a deterministic method will be preferred. Deterministic FRM methods enable the automatic correlation of facies in a large number of close-spaced wells, and prove useful when facies distribution is reasonably captured by dense well data coverage. On the other hand, if the aim is to recreate facies distribution from a more limited dataset, but according to a preconceived conceptual depositional model, then a stochastic method will be preferred.

2) When deterministic facies reconstruction methods are applied, the main choice of the method to be used is that of employing a continuous method for ordered facies distributions (i.e. truncated-based method), or a categorical method (i.e. indicator-based method) for non-ordered facies distributions. Markov chain analysis provides an objective test of facies ordering.

3) When stochastic facies modelling methods are used, choosing between the different techniques requires a series of decisions by the modeller. These should be based on the scale of the problem, the type and density of

available data, the objective of the model, and aimed to best reproduce the conceptual depositional model; some general ideas are provided in Fig. 5. Currently there are no objective unequivocal rules to justify them, and this must be based on the modellers' experience, or by comparing the resultant facies distribution with the real facies distribution, which for most cases is unknown.

Nowadays, the main limitation of FRM methods is that processes responsible for the resulting facies architecture are not included explicitly in the modelling algorithm. Process-based sedimentary models, formulating such processes explicitly, are currently most used to better understand the factors controlling sedimentary heterogeneity (Teles et al., 2001; Bitzer and Salas, 2002; Gratacós, 2004; Euzen et al., 2004; Burgess et al., 2006). However, these tools have not been widely applied for building facies distributions of the subsurface directly applicable for predictive and practical purposes because of: 1) the challenge of conditioning on hard data, 2) the complexity of inferring their input data parameters, and 3) their scale and temporal limitations. The next generations of FRM methods should be more process oriented, or at least to enable to widely benefit from the output of process-based methods in order to derive their input soft data. Obviously, such improvements will benefit from the increase in computing power and efficiency in database management during the forthcoming years.

ACKNOWLEDGEMENTS

The research was carried out in the Geomodels Institute. This Institute is sponsored by the Generalitat de Catalunya (DURSI) and by the Instituto Geológico y Minero de España (IGME) and includes the 3D Geological Modelling CER (University of Barcelona). The authors are indebted to ENDESA MINA PUENTES for providing the first dataset. Financial support from the Spanish Government (Dirección General de Investigación (Projects COMODES: CGL 2004-05816-C02-01/BTE and MARES: CGL 2004-05816-C02-02/BTE) and the Generalitat de Catalunya (Grup de Recerca de Geodinàmica i Anàlisi de Conques, 2005SGR-000397). Research by O. Falivene was funded by a pre-doctoral grant from the Spanish Government (Ministerio de Educación y Ciencia). Roxar is thanked for providing the IRAP RMS reservoir modelling software. This article summarizes part of the research included in the Thesis of O. Falivene (Testing three-dimensional facies reconstruction and modelling techniques applied to cored and outcropping analogues. Examples from swamp coal zones to alluvial fans and marine turbidite sequences, 2006, Universitat de Barcelona, 358 pp.); their reviewers are gratefully acknowledged. The original manuscript has been improved thanks to the comments by Dr. Ph. Renard (Univ. of Neuchatel), Dr. G. de Marsily (Univ. Pierre et Marie Curie), and Dr. R. Smith (Shell).

REFERENCES

Ahlberg, J.H., Nilson, E.W., Walsh, J.L., 1967. The theory of splines and its applications. New Cork, Academic Press, 280 pp.

Ainsworth, R.B., Sanlung, M., Duivenvoorden, T.C., 1999. Correlation techniques, perforation strategies and recovery factors: an integrated 3D reservoir modelling study, Sirikit field, Thailand. American Association of Petroleum Geologists Bullertin, 83, 1535-1551.

Alabert, F., 1987. The practice of fast conditional simulations through LU decomposition of the covariance matrix. Mathematical Geology, 19, 369-386.

Alexander, J., 1993. A discussion on the use of analogues for reservoir geology. In: Ashton, M. (ed.). Advances in Reservoir Geology. Geological Society Special Publication, 69, 175-194.

Arbués, P., Mellere, D., Falivene, O., Fernández, O., Muñoz, J.A., Marzo, M., de Gibert, J.M., in press. Context and architecture of the Ainsa-1-quarry channel complex. Ainsa Basin, Eocene South-Central Pyrenees, Spain. In: Nielsen, T.H., Shew, R.D., Steffens, G.S., Studlick, R.J. (eds.), in press. Atlas of Deep-Water Outcrops. American Association of Petroleum Geologist Studies in Geology, 56.

Arbués, P., Muñoz, J.A., Fernández, O., Falivene, O., Marzo, M., 2003. Contrasts on the 3D Geometry and Architecture of two Turbidite Systems in the Ainsa Basin. South-Central Pyrenees, Spain, American Association of Petroleum Geologists International Conference & Exhibition, Barcelona, Abstract, A4-A5.

Arbués, P., Muñoz, J.A., Poblet, J., Puigdefàbregas, C., McClay, K., 1998. Significance of submarine truncation surfaces in the sedimentary infill of the Ainsa basin (Eocene of south-central Pyrenees, Spain). 15th International Sedimentological Congres, Alicante, Spain, Publicaciones de la Universidad de Alicante, 145-146.

Artimo, A., Makinen, J., Berg, R.C., Abert, C.C., Salonen, V.P., 2003. Three-dimensional geologic modeling and visualization of the Virttaankangas aquifer, southwestern Finland. Hydrogeology Journal, 11, 378-386.

Bacelar, J., Alonso, M., Kaiser, C., Sánchez, M., Cabrera, L., Sáez, A., Santanach, P., 1988. La cuenca terciaria de As Pontes (Galicia): su desarrollo asociado a inflexiones contractivas de una falla direccional. II Congreso Geológico de España, Simposios, Granada, Sociedad Geológica de España, 113-121.

Beucher, H., Geffroy, F., Doligez, B., 2003. Complex features in sedimentology and truncated plurigaussian simulations. American Association of Petroleum Geologists Annual Convention, Salt Lake City (Utah), Extended Abstract.

Bitzer, K., Salas, R., 2002. SIMSAFADIM: three-dimensional simulation of stratigraphic architecture and facies distribution modeling of carbonate sediments. Computers and Geosciences, 28, 1177-1192.

Brandsaeter, I., Wist, H.T., Naess, A., Lia, O., Arnzten, O.J., Ringrose, P.S., Martinius, A.W., Lerdahl, R., 2001. Ranking stochastic realizations of complex tidal reservoirs using streamline simulation criteria. Petroleum Geoscience, 7, S53-S63.

Bridge, J.S., Mackey, S., 1993. A theoretical study of fluvial sandstone body dimensions. In: Flint, S.S., Bryant, I.D. (eds.). The Geologic Modelling of Hydrocarbon Reservoirs and Outcrop Analogues. International Association of Sedimentologists, Special Publications, 15, 213-236.

Bryant, I.D., Flint, S.S., 1993. Quantitative clastic reservoir geological modelling: problems and prespectives. In: Flint, S.S., Bryant, I.D. (eds.). The Geologic Modelling of Hydrocarbon Reservoirs and Outcrop Analogues. International Association of Sedimentologists, Special Publications, 15, 3-20.

Bryant, I.D., Carr, D., Cirilli, P., Drinkwater, N.J., McCormick, D., Tilke, P., Thurmond, J., 2000. Use of 3D digital analogues as templates in reservoir modelling. Petroleum Geoscience, 6, 195-201.

Burgess, P.M., Lammers, H., van Oosterhout, C., Granjeon, D., 2006. Multivariate sequence stratigraphy: Tackling complexity and uncertainty with stratigraphic forward modeling, multiple scenarios, and conditional frequency maps. American Association of Petroleum Geologists Bulletin, 90, 1883-1901.

Cabello, P., Cuevas, J.L., Ramos, E., 2007. 3D modelling of grain size distribution in quaternay in deltaic plain deposits (Llobregat Delta, NE Spain). Geologica Acta, 5(3), 231-244.

Cabrera, L., Hagemann, H.W., Pickel, W., Sáez, A., 1992. Caracterización Petrológica y Geoquímica Orgánica de los lignitos de la cuenca de As Pontes (La Coruña). II Congreso Geológico de España - VIII Congreso Latinoamericano de Geología, Salamanca, Tomo 2, 239-246.

Cabrera, L., Hagemann, H.W., Pickel, W., Sáez, A., 1995. The coal-bearing, Cenozoic As Pontes Basin (northwestern Spain): geological influence on coal characteristics. International Journal of Coal Geology, 27, 201-226.

Cabrera, L., Ferrús, B., Sáez, A., Santanach, P., Bacelar., J., 1996. Onshore Cenozoic strike-slip basins in NW Spain. In: Friend, P.F., Dabrio, C.J. (eds.). Tertiary Basins of Spain. The Stratigraphic Record of Crustal Kinematics. Cambridge, Cambridge University Press, 247-254.

Caers, J., 2001. Geostatistical reservoir modelling using statistical pattern recognition. Journal of Petroleum Science and Engineering, 29, 177-188.

Caers, J., Zhang, T., 2004. Multiple-point geostatistics: A quantitative vehicle for integrating geologic analogs into multiple reservoir models. In: Grammer, M., Harris, P.M., Eberli, G.P. (eds.). Integration of outcrop and modern analogs in reservoir modelling. American Association of Petroleum Geologists Memoir, 80, 383-394.

Carle, S.F., Fogg, G.E., 1996. Transition probability based indicator geostatistics. Mathematical Geology, 28, 453-476.

Carle, S.F., Fogg, G.E., 1997. Modeling spatial variability with one and multidimensional continuous-lag Markov chains. Mathematical Geology, 29, 891-917.

Carle, S.F., Labolle, E.M., Weissmann, G.S., Van Brocklin, D., Gogg, G.E., 1998. Conditional Simulation of Hydrofacies Architecture: A Transition Probability/Markov Approach. In: Fraser, G.S., Davis, J.M. (eds.). Hydrogeologic models of sedimentary aquifers, SEPM Special Publication, Concepts in Hydrogeology and Environmental Geology, 147-170.

Castellini, A., Chawathé, A., Larue, D., Landa, J.L., Jian, F.X., Toldi, J., 2003. What is Relevant to Flow? A Comprehensive Study Using a Shallow Marine Reservoir. Society of Petroleum Engineers Paper No. 79669, 12 pp.

Clark, J.D., Pickering, K.T., 1996. Architectural Elements and Growth Patterns of Submarine Channels: Application to Hydrocarbon Exploration. American Association of Petroleum Geologists Bulletin, 80, 194-221.

Clementsen, R., Hurst, A., Knarud, R., Omre, H., 1990. A computer program for evaluation of fluvial reservoirs. In: Buller, A.T., Berg, E., Hjemeland, O., Kleppe, J., Torsaeter, O., Aasen, J.O. (eds.). North Sea Oil and Gas Reservoirs II. London, Graham and Trotham, 373-385.

Conybeare, D.M., Cannon, S., Karaoguz, O., Uygur, E., 2004. Reservoir modelling of the Hamitabat Field, Thrace Basin, Turkey: an example of a sand-rich turbidite system. In: Lomas, S.A., Joseph, P. (eds.). Confined Turbidite Systems. Geological Society, London, Special Publications, 222, 307-320.

Cressie, N., 1990. The origins of kriging. Mathematical Geology, 22, 239-252.

Cunha, L.B., Barroso, A., Romeu, R.K., Sombra, C.L., Cortez, M.M., Backheuser, Y., Lopes, M.F., Scwerdesky, G., Bruhn, C.H., de Souza, R.S., Becker, M.R., 2001. A multi-scale approach to improve reservoir characterization and forecasting: the Albacora Field (deep-water offshore Brazil) study. Petroleum Geoscience, 7, S17-S23.

Dalrymple, M., 2001. Fluvial reservoir architecture in the Statfjord Formation (northern North Sea) augmented by outcrop analogue statistics. Petroleum Geoscience, 7, 115-122.

Davis, M., 1987. Production of conditional simulations via the LU decomposition of the covariance matrix. Mathematical Geology, 19, 91-98.

de Marsily, G., Delay, F., Teles, V., Schafmeister, M.T., 1998. Some current methods to represent the heterogeneity of natural media in hydrogeology. Hydrogeology Journal, 6, 115-130.

de Marsily, G., Delay, F., Gonçalves, J., Renard, P., Teles, V., Violette, S., 2005. Dealing with spatial heterogeneity. Hydrogeology Journal, 13, 161-183.

Delhomme, A.E.K., Giannesini, J.F., 1979. New reservoir description techniques improve simulation results in Hassi-Messaud field, Algeria. Society of Petroleum Engineers Paper No. 8435, 11 pp.

Deutsch, C.V., 2002. Geostatistical Reservoir Modeling. Applied Geostatistics Series, New York, Oxford University Press, 376 pp.

Deutsch, C.V., Cockerham, P., 1994. Practical considerations in the application of simulated annealing to stochastic simulation. Mathematical Geology, 26, 67-82.

Deutsch, C.V., Hewet, T.A., 1996. Challenges in Reservoir Forecasting. Mathematical Geology, 28, 829-842.

Deutsch, C.V., Journel, A.G., 1998. GSLIB: Geostatistical Software Linrary and User's Guide, 2nd edition. New York, Oxford University Press, Applied Geostatistics Series, 350 pp.

Deutsch, C.V., Tran, T.T., 2002. FLUVISIM: a program for object-based stochastic modeling of fluvial depostional systems. Computers and Geosciences, 28, 525-535.

Deutsch, C.V., Wang, L., 1996. Hierarchical Object-Based Stochastic Modeling of Fluvial Reservoirs. Mathematical Geology, 28, 851-880.

Dirks, K.N., Hay, J.E., Stow, C.D., Harris, D., 1998. High-resolution studies of rainfall on Norfolk Island Part II: interpolation of rainfall data. Journal of Hydrology, 208, 187-193.

Doligez, B., Granjeon, D., Joseph, P., Eschard, R., 1999. How can stratigraphic modeling help constrain geostatistical reservoir simulations? In: Harbaugh, J.W., Watney, W.L., Rankey, E.C., Slingerland, R., Goldstein, R.H., Franseen, E.K. (eds.). Numerical experiments in stratigraphy; recent advances in stratigraphic and sedimentologic computer simulations. Society for Sedimentary Geology Special Publication, 62, 239-244.

Dowd, P.A., Pardo-Igúzquiza, E., Xu, C., 2003. Plurigau: a computer program for simulating spatial facies using truncated plurigaussian method. Computers and Geosciences, 29, 123-141.

Dreyer, T., Falt, L.M., Hoy, T., Knarud, R., Steel, R., Cuevas, J.L., 1993. Sedimentary architecture of field analogues for reservoir information (SAFARI): a case study of the fluvial Escanilla Formation, Spanish Pyrenees. In: Flint, S., Bryant, I.D. (eds.). The geological modelling of hydrocarbon reservoirs and outcrop analogues. International Association of Sedimentologists, Special Publications, 15, 57-80.

Dubrule, O., 1984. Comparing Splines and Kriging. Computers and Geosciences, 10, 327-338.

Dubrule, O., 1994. Estimating or Choosing a Geostatistical Model? In: Dimitrakopoulos, R. (ed.). Geostatistics for the Next Century. Dordrecht, The Netherlands, Kluwer Academic Publishers, 3-14.

Dubrule, O., Damsleth, E., 2001. Achievements and challenges in petroleum geostatistics. Petroleum Geoscience, 7, S1-S7.

Dubrule, O., Haldorsen, H.H., 1986. Geostatistics for permeability estimation. In: Lake, L.W., Carroll, H.B. (eds.). Reservoir Characterization. Orlando, Academic Press, 223-247.

Eschard, R., Lemouzy, P., Bacchiana, C., Désaubliaux, G., Parpant, J., Smart, B., 1998. Combining sequence stratigraphy, geostatistical simulations and production data for modeling a fluvial reservoir in the Chamoy Field (Triasic, France). American Association of Petroleum Geologists Bulletin, 82, 545-568.

Euzen, T., Joseph, P., Du Fornel, E., Lesur, S., Granjeon, D., Guillocheau, F., 2004. Three-dimensional stratigraphic modelling of the Grès d'Annot system, Eocene-Oligocene, SE France. In: Joseph, P., Lomas, S. (eds.). Deep-water sedimentation in the Alpine Foreland Basin of SE France: New perspectives on the Grès d'Annot and related systems. Geological Society Special Publications, 221, 161-180.

Falivene, O., Arbués, P., Gardiner, A.R., Pickup, G.E., Muñoz, J.A., Cabrera, L., 2006a. Best-practice stochastic facies modeling from a channel-fill turbidite sandstone analog (the "Quarry Outcrop", Eocene Ainsa Basin, NE Spain). American Association of Petroleum Geologists Bulletin, 90, 1003-1029.

Falivene, O., Arbués, P., Howell, J., Fernández, O., Cabello, P., Muñoz, J.A., Cabrera, L., 2006b. A FORTRAN program to introduce field-measured sedimentary logs into reservoir modelling packages. Computers and Geosciences, 32,1519-1522.

Falivene, O., Arbués, P., Howell, J., Muñoz, J.A., Fernández, O., Marzo, M., 2006c. Hierarchical geocellular facies modelling of a turbidite reservoir analogue from the Eocene of the Ainsa Basin, NE Spain. Marine and Petroleum Geolgy, 23, 679-701.

Falivene, O., Cabrera, L., Sáez, A., 2006d. Reconstrucción geoestadística de facies en un abanico aluvial dominado por aportes lutíticos (Cuenca cenozoica de As Pontes, A Coruña). Predicción de la distribución de acuíferos en cuerpos arenosos. VI Congreso del Grupo Español del Terciario, Salamanca, Geo-Temas, 9, 79-82.

Falivene, O., Cabrera, L., Sáez, A., 2007. Optimum and robust 3D facies interpolation strategies in a heterogeneous coal zone (Tertiary As Pontes basin, NW Spain). International Journal of Coal Geology, 71(2-3), 185-208.

Falivene, O., Cabrera, L., Sáez, A., in press. Large to intermediate-scale aquifer heterogeneity in fine-grain dominated alluvial fans (Cenozoic As Pontes basin, NW Spain): Insight based on 3D reconstruction. Hydrogeology Journal.

Falkner, A., Fielding, C., 1993. Quantitative facies analysis of coal-bearing sequences in the Bowen Basin, Australia: applications to reservoir description. In: Flint, S.S., Bryant, I.D. (eds.). The Geologic Modelling of Hydrocarbon Reservoirs and Outcrop Analogues. International Association of Sedimentologists Special Publications, 15, 81-98.

Felletti, F., 2004. Statistical modelling and validation of correlation in turbidites: an example from the Tertiary Piedmont Basin (Castagnola Fm., Northern Italy). Marine and Petroleum Geology, 21, 23-39.

Fernández, O., 2004. Reconstruction of geological structures in 3D. An example from the southern Pyrenees. Doctoral thesis. Universitat de Barcelona, 321 pp.

Fernández, O., Muñoz, J.A., Arbués, P., Falivene, O., Marzo, M., 2004. 3-D reconstruction of geological surfaces: an example of growth strata and turbidite systems from the Ainsa basin (Pyrenees, Spain). American Association of Petroleum Geologists Bulletin, 88, 1049-1068.

Ferrús, B., 1998. Análisis de cuenca y relaciones tectónica-sedimentación en la cuenca de As Pontes (Galícia). Doctoral thesis. Universitat de Barcelona, 351 pp.

Flach, G.P., Hamm, L.L., Harris, M.K., Thayer, P.A., Haselow, J.S., Smits, A.D., 1998. A method for characterizing hydrogeologic heterogeneity using lithologic data. In: Fraser, G.S., Davis, J.M. (eds.). Hydrogeologic models of sedimentary aquifers, SEPM Special Publication, Concepts in Hydrogeology and Environmental Geology, 119-136.

Fogg, G.E., Noyes, C.D., Carle, S.F., 1998. Geologically-based model of heterogeneous hydraulic conductivity in an alluvial setting. Hydrogeology Journal, 6, 131-143.

Galli, A., Beucher, H., Le Loc'h, G., Doliguez, Group, H., 1994. The pros and cons of the truncated Gaussian method. In: Armstrong, M., Dowd, P.A. (eds.). Geostatistical Simulations. The Netherlands, Kluwer Academic Publishers, 217-233.

Gingerich, P.D., 1969. Markov Analysis of cyclic alluvial sediments. Journal of Sedimentary Petrology, 39, 330-332.

Gómez-Hernández, J., Srivastava, R.M., 1990. ISIM 3D: an ANSI-C three-dimensional and multiple indicator conditional simulation program. Computers and Geosciences, 16, 355-410.

Goovaerts, P., 1996. Stochastic Simulation of Categorical Variables Using a Classification Algorithm and Simulated Annealing. Mathematical Geology, 28, 909-921.

Goovaerts, P., 1999. Impact of the simulation algorithm, magnitude of ergodic fluctuations and number of realizations on the spaces of uncertainty of flow properties. Stochastic Environmental Research and Risk Assessment, 13, 161-182.

Gratacós, O., 2004. SIMSAFADIM-CLASTIC: Modelización 3D de transporte y sedimentación clástica subacuatica. Doctoral thesis. Universitat de Barcelona, 216 pp.

Gringarten, E., Deutsch, C.V., 2001. Variogram interpretation and modeling. Mathematical Geology, 33, 507-535.

Guardiano, F., Srivastava, R.M., 1993. Multivariate geostatistics: beyond bivariate moments. In: Soares, A. (ed.). Geostatistics-Troia 1. Dordrecht, Kluwer Academic Publications, 113–114.

Guardiola-Albert, C., Gómez-Hernández, J., 2001. Average length of objects generated by a binary random function: discretization effects and relation with the variogram parameters, geoENV III. The Netherlands, Kluwer Academic Publishers, 323-332.

Gundeso, R., Egeland, O., 1990. SESIMIRA; a new geological tool for 3D modelling of heterogeneous reservoirs. In: Buller, A.T., Berg, E., Hjemeland, O., Kleppe, J., Torsaeter, O., Aasen, J.O. (eds.). North Sea oil and gas reservoirs conference, Proceedings, 363-371.

Hagemann, H.W., Pickel, W., Cabrera, L., Sáez, A., 1997. Tertiary lignites of the As Pontes (NW Spain) - An example for composition of bright coal layers and its implications for formation. 9th International Conference on Coal Science, Essen, Alemania, Proceedings 1, 31-34.

Haldorsen, H.H., Chang, D.M., 1986. Notes on stochastic shales - from outcrop to simulation model. In: Lake, L.W., Carroll, H.B. (eds.). Reservoir Characterization. Orlando, Academic Press, 445-485.

Haldorsen, H.H., Chang, D.M., Begg, S.H., 1987. Discontinuous vertical permeability barriers: a challenge to engineers and geologists. North Sea Oil and Gas Reservoirs. London, UK, The Norwegian Institute of Technology, 127-151.

Haldorsen, H.H., Damsleth, E., 1990. Stochastic Modeling. Journal of Petroleum Geology, 42, 404-412.

Harbaugh, J.W., Bonham-Carter, G., 1970. Computer simulation in geology. New York, Willey and Sons, 575 pp.

Hatloy, A.S., 1994. Numerical facies modeling combining deterministic and stochastic methods. In: Yarus, J.M., Chambers, R.L. (eds.). Stochastic Modeling and Geostatistics: principles, methods and case studies. American Association of Petroleum Geologists, Computers Applications in Geology, 3, 109-120.

Hauge, R., Syverseveen, A.R., MacDonald, A.C., 2003. Modeling Facies Bodies and Petrophysical Trends in Turbidite Reservoirs. Society of Petroleum Engineers Paper No. 84053, 7 pp.

Heinz, J., Aigner, T., 2003. Hierarchical dynamic stratigraphy in various Quaternary gravel deposits, Rhine glacier area (SW Germany): implications for hydrostratigraphy. International Journal of Earth Sciences (Geol Rundsch), 92, 923-938.

Hirst, J.P.P., Blackstock, C., Tyson, S., 1993. Stochastic modelling of fluvial sandstone bodies. In: Flint, S.S., Bryant, I.D. (eds.). The Geologic Modelling of Hydrocarbon Reservoirs and Outcrop Analogues. International Association of Sedimentologists Special Publications, 15, 237-252.

Hodgetts, D., Drinkwater, N.J., Hodgson, D., Kavanagh, J., Flint, S., Keogh, K.J., Howell, J., 2004. Three dimensional geological models from outcrop data using digital collection techniques: an example from the Tanqua Karoo depocentre, South Africa. In: Curtis, A., Wood, R. (eds.). Geological Prior Information: Information Science and Engineering. Geological Society of London, Special Publications, 239, 57-75.

Holden, L., Hauge, R., Skare, O., Skorstad, A., 1998. Modeling of fluvial reservoirs with object models. Mathematical Geology, 30, 473-496.

Hornung, J., Aigner, T., 1999. Reservoir and aquifer characterization of fluvial architectural elemets: Stubensandstein, Upper Triassic, southwest Germany. Sedimentary Geology, 129, 215-280.

Huerta, A., 1998. Petrografía, Mineralogía y Geoquímica de los lignitos de la cuenca Oligo-Miocena de As Pontes (A Coruña): Control geológico sobre la calidad del carbon. Doctoral thesis. Universitat de Barcelona, 333 pp.

Huerta, A., 2001. Resumen de tesis Doctoral: Caracterización mineralógica y geoquímica de los lignitos de la cuenca Terciaria de As Pontes (Provincia de La Coruña). Acta Geológica Hispánica, 36, 183-186.

Huerta, A., Querol, X., Sáez, A., Cabrera, L., 1997. Mineralogy and Geochemistry of the As Pontes lignites (NW Spain): Relation with paleohydrological basin evolution. In: Hendry, J., Carey, P., Ruffell, A., Worden, R. (ed.). Migration and Interaction in Sedimentary basins and Orogenic Belts. GEOFLUIDS II'97. Contributions to the Second International Conference on Fluid Evolution. Belfast, Geological Society Special Publication, 370-373.

Huggenberger, P., Aigner, T., 1999. Introduction to the special issue on aquifer-sedimentology: problems, perspectives and modern approaches. Sedimentary Geology, 129, 179-186.

Hurst, A., Cronin, B., Hartley, A., 2000. Reservoir modelling of sand-rich deep-water clastics: the necessity of downscaling. Petroleum Geoscience, 6, 67-76.

Hurst, A., Verstralen, I., Cronin, B., Hartley, A., 1999. Sand-rich fairways in deep-water clastic reservoirs: genetic units, capturing uncertainty, and a new approach to reservoir modeling. American Association of Petroleum Geologists Bulletin, 83, 1096-1118.

Isaaks, E.J., Srivastava, R.M., 1989. An introduction to Applied Geostatistics. New York, Oxford University Press, 561 pp.

Jian, F.X., Larue, D., Castellini, A., Toldi, J., 2002. Reservoir Modeling Methods and Characterization Parameters For a Shoreface Reservoir: What is Important For Fluid Flow Performance? Society of Petroleum Engineers Paper No. 77428, 14 pp.

Johnson, N.M., Dreiss, S.J., 1989. Hydrostratigraphic interpretation using indicator geostatistics. Water Resources Research, 25, 2501-2510.

Jones, A., Doyle, J., Jacobsen, T., Kjonsvik, D., 1995. Which subseismic heterogeneities influence waterflood performance? A case study of a low net to gross fluvial reservoir. In Hahn, H.J. (ed.). New developments in improved oil recovery. Geological Society of London Special Publication, 84, 5-18.

Jones, T.A., 1988. Geostatistical Models with Stratigraphic Control - Short Note. Computers and Geosciences, 14, 135-138.

Jones, T.A., 1992. Extensions to Three Dimensions Introduction to the Section On 3-D Geologic Block Modeling. In: Hamilton, D.E., Jones, T.A. (eds.). Computer Modeling of Geologic Surfaces and Volumes. American Association of Petroleum Geologists, Computers Applications in Geology, 1, 175-182.

Jones, T.A., 2001. Using flowpaths and vector fields in object-based modeling. Computers and Geosciences, 27, 133-138.

Jones, T.A., Larue, D.K., 1997. Object-based modeling and deepwater depositional systems. In: Pawlowsky, V. (ed.). IAMG'97: Third annual conference of the International Association for Mathematical Geology, International Center for Numerical Methods in Engineering, Barcelona, Proceedings, 438-443.

Jones, T.J., Hamilton, D.E., Johnson, C.R., 1986. Contouring geologic surfaces with the computer. New York, Van Nostrand Reinhold, 314 pp.

Joseph, P., Hu, L.Y., Dubrule, O., Claude, D., Crumeyrolle, P., Lesseur, J.L., Soudet, H.J., 1993. The Roda deltaic complex (Spain): From sedimentology to reservoir stochastic modelling. In: Eschard, R., Doliguez, B. (eds.). Subsurface Reservoir Characterization from Outcrop Observations. Paris, Editions Technip, 97-109.

Journel, A.G., 1974. Geostatistics for conditional simulation of orebodies. Economic Geology, 69, 673-687.

Journel, A.G., 1983. Nonparametric Estimation of Spatial Distributions. Mathematical Geology, 15, 445-468.

Journel, A.G., 1985. The Deterministic Side of Geostatistics. Mathematical Geology, 17, 1-15.

Journel, A.G., 1986. Geostatistics: Models and Tools for the Earth Sciences. Mathematical Geology, 18, 119-140.

Journel, A.G., Alabert, F.G., 1989. Non-Gaussian data expansion in the earth sciences. Terra Nova, 1, 123-134.

Journel, A.G., Deutsch, C.V., 1993. Entropy and spatial disorder. Mathematical Geology, 25, 329-355.

Journel, A.G., Huijbregts, C.J., 1978. Mining geostatistics. London, Academic Press, 600 pp.

Journel, A.G., Isaaks, E.H., 1984. Conditional Indicator Simulation: Application to a Saskatchewan uranium deposit. Mathematical Geology, 16, 685-718.

Journel, A.G., Kyriakidis, P.C., Mao, S., 2000. Correcting the Smoothing Effect of Estimators: A Spectral Postprocessor. Mathematical Geology, 32, 787-813.

Journel, A.G., Rossi, M., 1989. When do we need a trend in kriging? Mathematical Geology, 21, 715-739.

Journel, A.G., Ying, Z., 2001. The theoretical links between Sequential Gaussian Simulation, Gaussian Truncated Simulation, and Probability Field Simulation. Mathematical Geology, 33, 31-39.

Journel, A.G., Gómez-Hernández, J.J., 1993. Stochastic Imaging of the Wilmington Clastic Sequence. Society of Petroleum Engineers Formation Evaluation March, 33-40.

Journel, A.G., Gundeso, R., Gringarten, E., Yao, T., 1998. Stochastic modelling of a fluvial reservoir: a comparative review of algorithms. Journal of Petroleum Science and Engineering, 21, 95-121

Kane, V.E., Begovich, C.L., Butz, T.R., Myers, D.E., 1982. Interpretation of Regional Geochemistry Using Optimal Interpolation Parameters. Computers and Geosciences, 8, 117-135.

Knudby, C., Carrera, J., 2005. On the relationship between indicators of geostatistical, flow and transport connectivity. Advances in Water Resources, 28, 405-421.

Koike, K., Shiraishi, Y., Verdeja, E., Fujimura, K., 1998. Three-Dimensionsal Interpolation and Lithofacies Analysis of Granular Composition Data for Eathquake-Engineering Characterization of Shallow Soil. Mathematical Geology, 30, 733-759.

Koltermann, C.E., Gorelick, S.M., 1996. Heterogeneity in sedimentary deposits: A review of structure-imitating, process-imitating, and descriptive approaches. Water Resources Research, 32, 2617-2658.

Krum, G.L., Johnson, C.R., 1993. A 3-D modelling approach for providing a complex reservoir description for reservoir simulations. In: Flint, S.S., Bryant, I.D. (eds.). The Geologic Modelling of Hydrocarbon Reservoirs and Outcrop Analogues. International Association of Sedimentologists Special Publications, 15, 253-258.

Kupfersberger, H., Deutsch, C.V., 1999. Methodology for Integrating Analog Geologic Data in 3-D Variogram Modeling. American Association of Petroleum Geologists Bulletin, 83, 1262-1278.

Lafuerza, S., Canals, M., Casamor, J.L., Devincenzi, J.M., 2005. Characterization of deltaic sediment bodies based on in situ CPT/CPTU profiles: A case study on the Llobregat delta plain, Barcelona, Spain. Marine Geology, 222-223, 497-510.

Langlais, V., Doyle, J.D., Sweet, M.L., Geehan, G., 1993. An additional geological input to SIS: the vertical organization of lithofacies. In: Eschard, R., Doliguez, B. (eds.). Subsurface Reservoir Characterization from Outcrop Observations. Paris, Editions Technip, 111-123.

Larue, D., 2004. Outcrop and waterflood simulation modeling of the 100-Foot Channel Complex, Texas and the Ainsa II Channel Complex, Spain: Analogs to multistory and multilateral channelized slope reservoirs. In: Gramer, M., Harris, P.M., Eberli, G.P. (Eds.). Integration of outcrop and modern analogs in reservoir modelling. American Association of Petroleum Geologists Memoir, 80, 337-364.

Larue, D., Friedmann, F., 2005. The controversy concerning stratigraphic architecture of channelized reservoirs and recovery by waterflooding. Petroleum Geoscience, 11, 131-146.

Larue, D., Legarre, H., 2004. Flow units, connectivity, and reservoir characterization in a wave-dominated deltaic reservoir: Meren reservoir, Nigeria. American Association of Petroleum Geologists Bulletin, 88, 303-324.

Le Loc'h, G., Galli, A., 1996. Truncated plurigaussian method: theoretical and practical points of view. Fifth International Geostatistics Congress, Wollongong, Australia, Kluwer academic publishers, Proceedings, 211-222.

Li, H., White, C.D., 2003. Geostatistical models for shales in distributary channel point bars (Ferron Sandstone, Utah): from ground-penetrating radar to three-dimensional flow modelling. American Association of Petroleum Geologists Bulletin, 87, 1851-1868.

Lia, O., Tjelmeland, H., Kjellesvik, L.E., 1996. Modeling of facies architecture by marked point models. Fifth International Geostatistics Congress, Wollongong, Australia, Kluwer Academic Publishers, Proceedings, 386-398.

Liu, Y., 2006. Using the Snesim program for multiple-point statistical simulation. Computers and Geosciences, 32, 1544-1563.

Liu, Y., Harding, A., Abriel, W., Strebelle, S., 2004. Multiple-point simulation integrating wells, three-dimensional seismic data, and geology. American Association of Petreoleum Geologists Bulletin, 88, 905-921.

MacDonald, A.C., Aasen, J.O., 1994. A Prototype Procedure for Stochastic Modeling of Facies Tract Distribution in Shoreface Reservoirs. In: Yarus, J.M., Chambers, R.L. (eds.). Stochastic modeling and geostatistics. American Association of Petroleum Geologists, Computers Applications in Geology, 3, 91-108.

MacDonald, A.C., Falt, L.M., Hektoen, A.L., 1998. Stochastic modeling of incised valley geometries. American Association of Petroleum Geologists Bulletin, 82, 1156-1172.

MacDonald, A.C., Halland, E.K., 1993. Sedimentology and shale modeling of a sandstone-rich fluvial reservoir; upper Statfjord Formation, Statfjord Field, Northern Sea. American Association of Petroleum Geologists Bulletin, 77, 1016-1040.

MacDonald, A.C., Hoye, T.H., Lowry, P., Jacobsen, T., Aasen, F.O., Grindheim, A.O., 1992. Stochastic flow unit modeling of a North-Sea coastal-deltaic reservoir. First Break, 10, 124-133.

Matheron, G., 1963. Principles of geostatistics. Economic Geology, 58, 1246-1266.

Matheron, G., 1973. The intrinsic random functions and their applications. Advances in applied probability, 5, 439-468.

Matheron, G., Beucher, H., de Fouquet, H., Galli, A., Gerillot, D., Ravenne, C., 1987. Conditional simulation of the geometry of fluvio-deltaic reservoirs. Society of Petroleum Engineers Paper No. 6753.

Mathieu, Y., Verdier, F., Houel, P., Delmas, J., Beucher, H., 1993. Reservoir heterogeneity in fluviatile Keuper facies: a subsurface and outcrop study. In: Eschard, R., Doliguez, B. (eds.), Subsurface Reservoir Characterization from Outcrop Observations. Paris, Editions Technip, 145-160.

Mao, S., Journel, A.G., 1999. Conditional simulation of lithofacies with 2D seismic data. Computers and Geosciences, 25, 845-862.

Miall, A.D., 1973. Markov Analysis applied to an ancient alluvial plain succession. Sedimentology, 20, 347-364.

Miall, A.D., 1991. Hierarchies of architectural units in terrigenous clastic rocks, and their relationship to sedimentation rate. In: Miall, A.D., Tyler, N. (eds.). The three-dimensional facies architecture of terrigenous clastics sediments and its implications for hydrocarbon discovery and recovery. SEPM Concepts in Sedimentology and Palaentology, 3, 6-11.

Mijnssen, F.C.J., 1997. Modelling of sandbody connectivity in the Schooner Field. In: Ziegler, K., Turner, P., Daines, S.R. (eds.). Petroleum geology of the southern North Sea: future potential. Geological Society Special Publication, 123, 169-180.

Mitasova, H., Hofierka, J., 1993. Interpolation by regularized spline with tension: II. Application to Terrain Modeling and Surface Geometry Analysis. Mathematical Geology, 25, 657-669.

Mitasova, H., Mitas, L., 1993. Interpolation by regularized spline with tension: I. Theory and implementation. Mathematical Geology, 25, 641-655.

Muñoz, J.A., Arbués, P., Serra-Kiel, J., 1998. The Ainsa basin and the Sobrarbe oblique thrust system: Sedimentological and tectonic processes controlling slope and platform sequences deposited synchronously with a submarine emergent thrust system. In: Meléndez Hevia, A., Soria, A.R. (eds.). 15th International Association of Sedimentologists International Congress of Sedimentology, Alicante, Field trip guidebook, 213-223.

Mutti, E., 1985. Hecho Turbidite Syste, Spain. In: Bouma, A., Normark, W.R., Barnes, N.E. (eds.). Submarine fans and related turbidite systems. Frontiers in Sedimentary Geology. New York, Springer, 205-208.

Mutti, E., Normark, W.R., 1987. Comparing examples of modern and ancient turbidite systems: Problems and Concepts. In: Legget, J.K., Zuffa, G.G. (eds.). Deep water clastic deposits: Models and Case Histories, London, Graham and Trotman ed., 1-38.

Mutti, E., Seguret, M., Sgavetti, M., 1988. Sedimentation and deformation in the Tertiary Sequences of the Southern Pyrenees. AAPG Mediterranean Basins Conference, Nice, France, Special Publication of the Institute of Geology of the University of Parma, Field Trip 7 guidebook, 153 pp.

Novakovic, D., White, C.D., Corbeanu, R., Hammon III, W.S., Bhattacharya, J., McMechan, G.A., 2002. Hydraulic Effects of Shales in Fluvial-Deltaic Deposits: Ground-Penetrating Radar, Outcrop Observations, Geostatistics and Three-Dimensional Flow Modeling for the Ferron Sandstone, Utah. Mathematical Geology, 34, 857-893.

Olea, R., Pawlowsky, V., 1996. Compensating for estimation smoothing in kriging. Mathematical Geology, 28, 407-417.

Pebesma, E.J., Wesseling, C.G., 1998. GSTAT: A program for geostatistical modelling, prediction and simulation. Computers and Geosciences, 24, 17-31.

Pringle, J.K., Westerman, A.R., Clark, J.D., Drinkwater, N.J., Gardiner, A.R., 2004. 3D high-resolution digital models of outcrop analogue study sites to constrain reservoir model uncertainty: an example from Alport Castles, Derbyshire, UK. Petroleum Geoscience, 10, 343-352.

Purvis, K., Kao, J., Henderson, J., Duranti, D., 2002. Complex reservoir geometries in a deep-water clastic sequence, Gryphon Field, UKCS: injection structures, geological modelling and reservoir simulation. Marine and Petroleum Geology, 19, 161-179.

Pyrcz, M.J., Catuneanu, O., Deutsch, C., 2005. Stochastic surface-based modeling of turbidite lobes. American Association of Petroleum Geologists Bulletin, 89, 177-191.

Ringrose, P.S., Nordahl, K., Wen, R., 2005. Vertical permeability estimation in heterolithic tidal sandstones. Petroleum Geoscience, 11, 29-36.

Ritzi, R.W., 2000. Behaviour of indicator variograms and transition probabilities in relation to the variance in lengths of hydrofacies. Water Resources Research, 36, 3375-3381.

Ritzi, R.W., Dominic, D.F., Brown, N.R., Kausch, K.W., McAlenney, P.J., Basial, M.J., 1995. Hydrofacies distribution and correlation in the Miami Valley aquifer system. Water Resources Research, 31, 3271-3281.

Robinson, J.W., McCabe, P.J., 1997. Sandstone-Body and Shale-Body Dimensions in a Braided Fluvial System: Salt Wash Sandstone Member (Morrison Formation), Garfield County, Utah. American Association of Petroleum Geologists Bulletin, 81, 1267-1291.

Ross, M., Parent, M., Lefebvre, R., 2005. 3D geologic framework models for regional hydrogeology and land-use management: a case study from a Quaternary basin of southwestern Quebec, Canada. Hydrogeology Journal, 6-7, 690-707.

Rudkiewicz, J.L., Guérillot, D., Galli, A., Heresim, G., 1990. An integrated software for stochastic modeling of reservoir lithology and property with an example from the Yorkshire Middle Jurassic. In: Butler, A.T., Berg, E., Hjemeland, O., Kleppe, J., Torsaeter, O., Aasen, J.O. (eds.). North Sea oil and gas reservoirs II. London, Graham and Trotman, 399-406.

Santanach, P., Baltuille, J.M., Cabrera, Ll., Monge, C., Sáez, A., Vidal-Romaní, J.R., 1988. Cuencas terciarias gallegas relacionadas con corredores de fallas direccionales. II Congreso Geológico de España, Simposios, Granada, Sociedad Geológica de España, 123-133.

Santanach, P., Ferrús, B., Cabrera, L., Saez, A., 2005. Origin of a restraining bend in an evolving strike-slip system: The Cenozoic As Pontes basin (NW Spain). Geologica Acta, 3, 225-239.

Satur, N., Keeling, G., Cronin, B.T., Hurst, A., Gurbuz, K., 2005. Sedimentary architecture of a canyon-style fairway feeding a deep-water clastic system, the Miocene Cingoz Formation, southern Turkey: significance for reservoir characterisation and modelling. Sedimentary Geology, 173, 91-119.

Scheibe, T., Freyberg, D.L., 1995. Use of sedimentological information for geometric simulation of natural porus media structure. Water Resources Research, 31, 3259-3270.

Schuppers, J.D., 1993. Quantification of turbidite facies in a reservoir-analogous submarine-fan channel sandbody, south-central Pyrenees, Spain. In: Flint, S.S., Bryant, I.D. (eds.). The Geologic Modelling of Hydrocarbon Reservoirs and Outcrop Analogues. Special Publications of the International Association of Sedimentologists, 15, 99-112.

Schuppers, J.D., 1995. Characterization of Deep-Marine Clastic Sediments from Foreland Basins: Outcrop-derived concepts for exploration, production and reservoir modelling. Doctoral Thesis. Delft University of Technology, The Netherlands, 272 pp.

Seifert, D., Jensen, J.L., 1999. Using Sequential Indicator Simulation as a tool in reservoir description: Issues and Uncertainties. Mathematical Geology, 31, 527-550.

Seifert, D., Jensen, J.L., 2000. Object and Pixel-based reservoir modeling of a Braided Fluvial Reservoir. Mathematical Geology, 32, 581-603.

Skorstad, A., Hauge, R., Holden, L., 1999. Well conditioning in a fluvial reservoir model. Mathematical Geology, 31, 857-872.

Smith, R., Møller, N., 2003. Sedimentology and reservoir modelling of the Ormen Lange field, mid Norway. Marine and Petroleum Geology, 20, 601-613.

Smith, R.D.A., Ecclestone, M. 2006. Multiscale 3D Interpretation and modelling for exploration and on down the lifecycle stream. GCSSEPM, Houston.

Srivastava, R.M., 1994. An overview of stochastic methods for reservoir characterization. In: Yarus, J.M., Chambers, R.L. (eds.). Stochastic Modeling and Geostatistics: principles, methods and case studies, American Association of Petroleum Geologists, Computers Applications in Geology, 3, 3-16.

Stanley, K.O., Jorde, K., Raestad, N., Stockbridge, C.P., 1990. Stochastic modelling of reservoir sandbodies for input to reservoir simulation, Snorre field, northern North Sea, Norway.

In: Buller, A.T., Berg, E., Hjemeland, O., Kleppe, J., Torsaeter, O., Aasen, J.O. (eds.). North Sea Oil and Gas Reservoirs II. London, Graham and Trotham, 91-101.
Stephen, K.D., Clark, J.D., Pickup, G.E., 2002. Modeling and Flow Simulations of a North Sea Turbidite Reservoir: Sensitivities and Upscaling. Society of Petroleum Engineers Paper No. 78292, 15 pp.
Strebelle, S., 2002. Conditional Simulation of Complex Geological Structures Using Multiple-Point Statistics. Mathematical Geology, 34, 1-22.
Strebelle, S., Journel, A., 2001. Reservoir Modeling Using Multiple-Point Statistics. Society of Petroleum Engineers Paper No. 71324, 11 pp.
Strebelle, S., Payrazyan, K., Caers, J., 2002. Modeling a Deepwater Turbidite Reservoir conditional to seismic data using multiple-point geostatistics. Society of Petroleum Engineers Paper No. 77425, 10 pp.
Sweet, M.L., Blewden, C.J., Carter, A.M., Mills, C.A., 1996. Modeling heterogeneity in a low permeability gas reservoir using geostatistical techniques, Hyde Field. American Association of Petroleum Geologists Bulletin, 80, 1719-1735.
Teegavarapu, R.S.V., Chandramouli, V., 2005. Improved weighting methods, deterministic and stochastic data-driven models for estimation of missing precipitation records. Journal of Hydrology, 312, 191-206.
Teles, V., Bravard, J.P., de Marsily, G., Perrier, E., 2001. Modelling of the construction of the Rhône alluvial plain since 15000 years BP. Sedimentology, 48, 1209-1224.
Tetzlaff, D.M., Harbaugh, J.W., 1989. Simulating Clastic Sedimentation. New York, Van Nostrand Reinhold, 202 pp.
Tompson, A.F.B., Ababou, R., Gelhar, L.W., 1989. Implementation of the three-dimensional turning bands field generator. Water Resources Research, 25, 2227-2243.
Tran, T.T., 1994. Improving variogram reproduction on dense simulation grids. Computers and Geosciences, 20, 1161-1168.
Tye, R.S., 2004. Geomorphology: An approach to determining subsurface reservoir dimensions. American Association of Petroleum Geologists Bulletin, 88, 1123-1147.
Tyler, K., Henriquez, A., MacDonald, A.C., Svanes, T., Hoilden, L., Kektoen, A.L., 1994a. Moheres -A Collection of Stochastic Models for Describing Heterogeneities in Clastic Reservoirs. In: Aasen, J.O. et al. (eds.). North Sea Oil & Gas Reservoirs III. Dordrecht, The Netherlands, Kluwer, 213-221.
Tyler, K., Henriquez, A., Svanes, T., 1994b. Modeling heterogeneities in fluvial domains, a review on the influence on production profile. In: Yarus, J.M., Chambers, R.L. (eds.). Stochastic Modeling and Geostatistics: principles, methods and case studies. American Association of Petroleum Geologists, Computers Applications in Geology, 3, 77-89.
van de Graaff, W.J.E., Ealey, P.J., 1989. Geological modeling for simulation studies. American Association of Petroleum Geologists Bulletin, 73, 1436-1444.
Viseur, S., Shutka, A., Mallet, J.L., 1998. New Fast, Stochastic, Boolean Simulation of Fluvial Deposits. Society of Petroleum Engineers Paper No. 49281, 13 pp.
Wadsley, A.W., Erlandsen, S., Goemans, H.W., 1990. HEX - A tool for integrated fluvial architecture modelling and numerical simulation of recovery process. In: Buller, A.T., Berg, E., Hjemeland, O., Kleppe, J., Torsaeter, O., Aasen, J.O. (eds.). North Sea Oil and Gas Reservoirs II. London, Graham and Trotham, 387-397.
Wang, L., 1996. Modeling complex reservoir geometries with multipoint statistics. Mathematical Geology, 28, 895-908.
Webb, E.K., Davis, J.M., 1998. Simulation of the spatial heterogeneity of geologic properties: an overview. In: Fraser, G.S., Davis, J.M. (eds.). Hydrogeologic models of sedimentary aquifers. SEPM Special Publication, Concepts in Hydrogeology and Environmental Geology, 1, 1-24.
Weber, D.D., Englund, E.J., 1992. Evaluation and comparison of spatial interpolators. Mathematical Geology, 24, 381-391.
Weber, D.D., Englund, E.J., 1994. Evaluation and comparision of spatial interpolators II. Mathematical Geology, 26, 589-603.
Weber, K.J., 1986. How heterogeneity affects oil recovery. In: Lake, L.W., Carroll, H.B. (eds.). Reservoir Characterization. Orlando, Academic Press, 445-485.
Weber, K.J., van Geuns, L.C., 1990. Framework for constructing clastic reservoir simulation models. Journal of Petroleum Technology, 42, 1248-1253.
Weissmann, G.S., Fogg, G.E., 1999. Multi-scale alluvial fan heterogeneity modeled with trasition probability geostatistics in a sequence stratigraphic framework. Journal of Hydrology 226, 48-65.
Weissmann, G.S., Carle, S.F., Fogg, G.E., 1999. Three-dimensional hydrofacies modeling based on soil surveys and transition probability geostatistics. Water Resources Research, 35, 1761-1770.
Weissmann, G.S., Zhang, Y., Labolle, E.M., Fogg, G.E., 2002. Dispersion of groundwater age in an alluvial aquifer system. Water Resources Research 38, 1198-1211.
Willis, B.J., White, C.D., 2000. Quantitative outcrop data for flow simulation. Journal of Sedimentary Research, 70, 788-802.
Yamamoto, J.K., 2005. Correcting the Smoothing Effect of Ordinary Kriging Estimates. Mathematical Geology, 37, 69-94.
Yao, T., 2002. Integrating Seismic Data for Lithofacies Modeling: A Comparison of Sequential Indicator Simulation Algorithms. Mathematical Geology, 34, 387-403.
Zimmerman, D., Pavlik, C., Ruggles, A., Armstrong, P., 1999. An experimental comparison of ordinary and universal kriging and inverse distance weighting. Mathematical Geology, 31, 375-390.
Zoraster, S., 1996. Imposing Geologic Interpretations on Computer-Generated Contours Using Distance Transformation. Mathematical Geology, 28, 969-985.

Manuscript received June 2006;
revision accepted February 2007.